


RESEARCH ARTICLE

Condensation water in heritage touristic caves: Isotopic and hydrochemical data and a new approach for its quantification through image analysis

Cristina Liñán^{1,2}  | José Benavente³ | Yolanda del Rosal¹ | Iñaki Vadillo² | Lucía Ojeda² | Francisco Carrasco²

¹Research Institute, Nerja Cave Foundation. Carretera de Maro, Malaga, Spain

²Centre of Hydrogeology of University of Malaga, Department of Geology, Faculty of Science, University of Malaga, Malaga, Spain

³Department of Geodynamics-Water Research Institute, Faculty of Science, University of Granada, Granada, Spain

Correspondence

Cristina Liñán, Research Institute, Nerja Cave Foundation. Carretera de Maro s/n, 29787, Nerja, Malaga, Spain.
Email: cbaena@cuevadenerja.es

Abstract

Condensation water is a major factor in the conservation of heritage caves. It can cause dissolution of the rock substrate (and the pigments of rock art drawn on it) or covering thereof with mineral components, depending on the chemical saturation degree of the condensation water. In show caves, visitors act as a source of CO₂ and thus modify the microclimate, favouring negative processes that affect the conservation of the caves. In spite of their interest, studies of the chemical composition of this type of water are scarce and not very detailed. In this work we present research on the condensation water in the Nerja Cave, one of the main heritage and tourist caves in Europe. The joint analysis of isotopic, hydrochemical, mineralogical and microbiological data and the use of image analysis have allowed us to advance in the knowledge of this risk factor for the conservation of heritage caves, and to demonstrate the usefulness of image analysis to quantify the scope of the possible corrosion condensation process that the condensation water could be producing on the bedrock, speleothem and rock art. To our knowledge, this application of image analysis (relative to the condensation water in caves) is the first one of this type that has been documented.

KEYWORDS

cave conservation, corrosion condensation, hydrochemistry, image analysis, isotope, microbial community, Nerja Cave, nitrate contents

1 | INTRODUCTION

In caves, the air water vapour content influences the air density and, consequently, the airflows and the gas exchange between the exterior and interior atmospheres. It also influences phase-change processes between the vapour and liquid phases. Under natural conditions, an equilibrium exists between water vapour evaporation and condensation, which is determined by the vapour pressure that is in turn dependent on the temperature. The assumption is that, at the surface of cave walls and speleothems there is a boundary layer of saturated air that has the same temperature as the surface. This boundary layer

interacts with the surrounding air, causing condensation or evaporation of condensate in a dynamic relationship that is driven largely by the vapour gradient (De Freitas & Schmekal, 2003). Condensation per se is a dynamic process of moisture flux that might vary from hour to hour and for any given time period. The process can involve both condensation and evaporation of the condensate, depending on the direction of the vapour gradient between the air and the moist surface. When the amount of condensation over a given period exceeds the evaporation of condensate over that same period, condensation is observed to have occurred. Condensation water will accumulate if this condition re-occurs; otherwise it will dissipate (De Freitas &

Schmekal, 2003). The condensation process needs condensation nuclei, such as the roof, floor or walls of the cavity, the speleothems or even microscopic particles suspended in the air, such as dust or aerosols. In the latter case, the phenomenon is called “cave fog” (Badino, 2004). The condensation process used to be more evident in the areas nearest to the entrances of the caves—where the microclimates are more unstable—, showing characteristic macro-, meso- and micro-morphologies (James et al., 1982). Condensation corrosion in speleogenesis has been regarded as responsible for dissolutional modification during later stages of cave development of coastal (Tarhule-Lips & Ford, 1998) and hypogenic caves (Hill, 1987; Palmer & Palmer, 2000).

Condensation water intervenes in several processes related to cave conservation, especially when these contain heritage elements such as rock art or delicate speleothems (Fernández-Cortés et al., 2006). Condensation of the undersaturated water (contained in the minerals of the substrate on which it will be deposited) on the bedrock or speleothems in contact with CO₂-rich air can produce their dissolution. This is the process known as “corrosion condensation” (Dreybrodt et al., 2005). If the condensed water on the rock or speleothems subsequently evaporates and/or is degassed in response to a change in cave air PCO₂ to lower values, precipitation of the mineral dissolved in the water occurs, causing micro crystalline deposits or veils to appear and cover the rocky surface (Istvan & Micle, 1994). These condensation-evaporation cycles increase the condensation corrosion process (De Freitas & Schmekal, 2006). The condensation of water can also produce the mobilization and leaching of rock art pigments (Hoyos et al., 1998; Morat & Le Mouël, 1992).

Visitors to show caves can favour these processes, as they trigger changes in the temperature and humidity of the cave air, in the microbiology of the cave and, particularly, in the air CO₂ concentration. All these factors intervene in the dissolution-precipitation processes of bedrock/speleothems (Avramidis et al., 2001; De Freitas & Schmekal, 2006; Dublyansky & Dublyansky, 2000; Fernández-Cortés et al., 2006). The emission of water vapour released by visitors can induce water condensation in the cave. If the cave air is saturated in water vapour and the cave air temperature increases due to the entry of visitors, the maximum water content that the air can contain will increase momentarily. Part of the water vapour that people are emitting at first becomes part of the air, increasing its absolute humidity. But, when the visitors leave the cave, the cave air temperature begins to recover, decreasing until it reaches its natural values, and condensation processes take place. The CO₂ exhaled by the visitors increases the cave air PCO₂ and water PCO₂, as the gas dissolves in it. Higher PCO₂ levels cause higher acidity of the condensed water along the cave walls and higher temperatures support faster reaction rates (Vieten et al., 2016), increasing the carbonate dissolution rate during the period of visitation.

Visitor-induced corrosion processes can be significant in some cases. In Altamira Cave, Spain (one of the most important prehistoric heritage caves in the world, with exceptional rock paintings), Sánchez-Moral et al. (1999) calculated that visitor-induced corrosion was between 80 and 250 times greater than produced by natural

condensation processes. Vieten et al. (2016) studied the visitor-induced condensation corrosion in two caves of Mona Island (Puerto Rico) and calculated theoretical dissolution rates up to 50% higher in the presence of visitors (30 people) than compared to natural conditions. These results highlight the need to study the condensation process in tourist caves, to determine its impact on the conservation of speleothems and rock art.

In the last decades, numerous studies of condensation processes in caves have been published, based on their direct and indirect measurement (Auler & Smart, 2004; Cailhol et al., 2019; Calaforra et al., 1993; Cigna & Forti, 1986; De Freitas & Schmekal, 2003, 2006; Dublyansky & Dublyansky, 1998; Fairbridge, 1968; Galdenzi, 2012; Gázquez et al., 2015; Martín-García et al., 2010; Prokofiev, 1964; Sanna et al., 2015; Sarbu & Lascu, 1997, among others). The majority of these studies focused on estimating rates of condensation corrosion (natural or visitor-induced) or the amount of condensate accumulated in caves, in order to show their effects on cave morphology or speleogenesis or to provide explanatory models of the process itself.

Nevertheless, few studies exist in the literature that deal with the chemical composition of condensed water (probably due to the difficulty of its sampling), the spatial variation of condensation throughout large caves or its spatio-temporal variation. Different research reported by Dublyansky and Dublyansky (2000) have compiled data about the Total Dissolved Solid (TDS) of condensation waters corresponding to drops (average TDS: 22 mg/L) and trails and films (average TDS: 140 mg/L) sampled on the ceiling and the walls of caves of different karst massifs of Eurasia. Some tables annexed to the work of Cuezva (2008) reported hydrochemical data of condensed water on the ceiling of Altamira Cave, but provided no associated comments. Other available data come from induced condensation water collected on cleaned cool artificial surfaces such as ice-filled containers, although they are also very scarce. Homza et al. (1970) refer low TDS values, of about 8 mg/L, in such samples (Ochtinskaya Aragonite Cave, Slovakia). In induced condensates in caves of Cayman Brac (Caribbean Sea) Tarhule-Lips and Ford (1998) reported calcite saturation indices ranged from -1.06 (water strongly undersaturated with respect to calcite, capable of dissolving speleothem calcite) to $+0.88$ (supersaturated with respect to calcite water that would deposit new calcite upon them). In Praileaitz Cave (N of Spain), Vadillo (2010) reported undersaturated induced condensation water (calcite and aragonite saturation indices of -0.73 and -0.87 , respectively) with an average electrical conductivity value of 160 $\mu\text{S}/\text{cm}$, and with average values of the major ionic constituents of less than 7 mg/L, except those of HCO₃⁻ (89 mg/L) and Ca²⁺ (30 mg/L).

This study addresses the following objectives: firstly, on a global scale, to identify and understand the hydrological processes that condensation water induces on the cave substrate and, particularly, the corrosion condensation process, which can damage valuable heritage elements as rock art and speleothems. For this, we present the isotopic and hydrochemical data of 7 rainwater samples and 31 condensation water samples (natural and induced) collected from 2013 to 2018 in Nerja Cave and its surroundings (S of Spain), one of the most important prehistoric and touristic caves in Europe (Jordá et al., 2011;

Quiles et al., 2014). Additionally, we present the mineralogical analysis of the rock substrate and microbiological data of two biofilms developed on it, with the aim of identifying the possible origin of some anomalous nitrate concentrations found in the condensation water.

Secondly, we show the applicability of image analysis as a methodology to quantify the spatio-temporal variation of the condensation water area and the corrosion process. Image analysis, or photo-monitoring, has been used in studies related to the conservation of heritage sites (Rogerio-Candelera et al., 2008; Thornbush & Viles, 2008) but, to the best of our knowledge, this is the first documented case of the application of image analysis with this aim.

Hydrochemistry and spatio-temporal evolution of the condensation water over the rock substrate, are considered key aspects in the possible mineral corrosion/precipitation process, and thus it is of

concern with regard to the management of show caves and the conservation of their natural and cultural heritage.

2 | SITE DESCRIPTION

The Nerja Cave (NC) is located in the south of the Iberian Peninsula (Malaga province, Andalusia Region), in an area of great environmental value, between the Sierras de Tejeda, Almijara and Alhama Natural Park and the Protected Natural Landscape of the coastal cliffs of Maro-Cerro Gordo. It is one of the biggest and most important tourist caves in Spain, with about 4800 m of passages and an average of slightly more than 400 000 visitors annually. The cavity covers an area of 35 000 m² and has three natural entrances (E1, E2, E3 in Figure 1

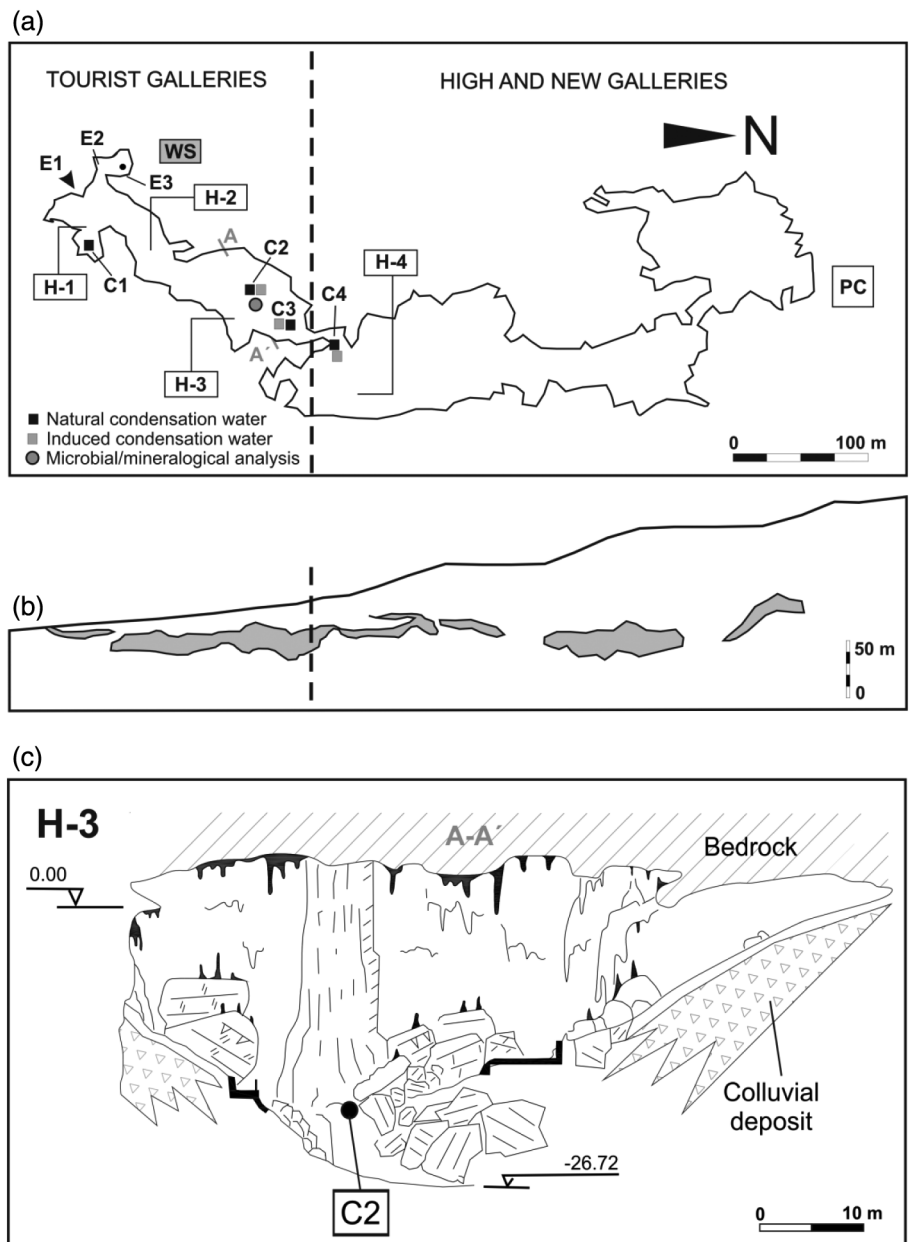


FIGURE 1 (a) Map of the Nerja Cave with the location of the control areas for the study of the condensation water (C1, C2, C3, C4). PC: Pintada Cave approximate location; WS: Weather station approximate location. E1: Tourist entrance; E2 and E3: Sinkholes. (b) Longitudinal cross-section of Nerja Cave, modified from Jiménez de Cisneros et al. (2020). The grey areas correspond to the cave. (c) Cross-section A-A' (Tourist galleries, chamber H-3), modified from Aranburu et al. (2019). The location of control area C2 is included. The minimum level of the cave (-26.72 m with respect to the entrance E1) is located in this chamber

(a). Its development is practically horizontal, lying between 123 and 191 m a.s.l. (Figure 1(b)). About a third of the cave, the so-called Tourist Galleries, has been opened to visitors since 1960, whilst the other sections, the High Galleries and New Galleries, are only accessible for scientific purposes and cave conservation activities. The cave has a network of monitoring stations arranged longitudinally, consisting of data-loggers featuring special sensors to record hourly measurements of air temperature, relative humidity, CO₂ concentration, pressure, air speed, and airflow direction, among other parameters (Liñán et al., 2018). Bedrock thickness above the cave varies from 4 to 50 m in the area opened to tourism, exceeding 80 m in the non-visitable area of the cave, according to the elevation of the topographic surface.

Cave development occurs in the unsaturated zone of the Sierra Almijara carbonate aquifer, made up of highly fractured Triassic dolomitic marbles of the Almijara Unit (Andreo et al., 2018). In 1991 a weather station (WS in Figure 1(a)) was installed a few meters from the Nerja Cave entrance to record external atmospheric parameters and for chemical and isotopic monitoring of the rainwater. The climate in the study area is coastal Mediterranean, with an average precipitation slightly below 500 mm/yr. The monthly average temperature ranges from about 13°C in January to 26°C in August, with a mean annual temperature and relative atmospheric humidity of 18.5°C and 66%, respectively (Liñán et al., 2007). A significant portion of the carbonate outcrops in this area is bare rock; soil cover is scarce, patchy and rarely exceeding thicknesses of 15 cm. The natural vegetation consists mainly of shrubs and pine trees. Rainfall infiltrates through fissures and fractures in the marbles, and drips from the roof of the cave. Slow water infiltration, with a lag of about 8 months between the input of rainfall and the output of seepage within the cave, prevails through most of the year, while “rapid” infiltration across epikarst and the unsaturated zone, with a lag shorter than 1–3 months, only occurs after significant recharge episodes (Andreo et al., 2002; Liñán et al., 1999).

The natural ventilation of the Nerja Cave karst system is clearly determined by variations in the density differences between the external and internal air. Four ventilation regimes (winter, spring, summer and autumn) and two ventilation modes with opposite airflow directions (upward airflow, UAF-mode; downward airflow, DAF-mode) have been defined during the annual cycle (Liñán et al., 2018; Liñán et al., 2020). During the winter regime, maximum ventilation exists and the airflow directions are normally from the lowest entrances of the NC to the highest entrances (UAF-mode). During the summer regime, ventilation is the lowest of the annual cycle and a reversed airflow pattern exists: cave air is expelled through the lowest entrances and external air is sucked in through the highest entrances (DAF-mode). The transitional ventilation regimes—spring and autumn—are the most complex, with changing air-flow directions of a diurnal or poly-diurnal periodicity.

Hydrogeological studies have been conducted in Nerja Cave since 1991 to characterize the rainwater and the drip water within the cavity and to determine the hydrodynamic functioning of the unsaturated zone of the aquifer in which it lies. However, the study of the

condensation water is much more recent, despite its importance for the conservation of the cave and its rocks paintings. In the Nerja Cave, condensation water is not observed during the entire year, as it appears and disappears seasonally. So far, condensation water has only been observed in three areas (C1, C2, C3 in Figure 1(a)) located in two chambers of the Tourist Galleries and in one of the High Galleries (C4 in Figure 1(a)). C1 is located on the ceiling of chamber H-2—one of the chambers nearest to the tourist entrance—about 9 m over the tourist trail; C2 is located in H-3, the more inner chamber of the Tourist Galleries. In this area, condensation water is visible from June to early November, on the ceiling and walls of a relatively small and isolated “room” located under a colossal column (32 m high and 18 m in diameter) and delimited by fallen blocks of bedrocks and speleothems (Figure 1(c)); C3 is also located in H-3 but in this case the condensation water is visible on the walls of a small room where a connection with the High Galleries is located, although this is not accessible to visitors. In C3, the surface occupied by the condensation water is very reduced (magnitude of cm²) but in C1 and C2, condensation water occupies a surface of several m². Very locally, some drops of condensation water have been observed in the first chamber of the High Galleries (H-4), on a wall with rock art (C4 in Figure 1(a)). White powdery patches on speleothems and bedrock are observed in the entire cave, some of them over rock art panels, that could correspond to mineral deposits associated with evaporation-condensation cycles and/or biofilms (Cañaveras et al., 2001; Dublyansky & Spötl, 2014).

3 | MATERIAL AND METHODS

3.1 | Rainwater and condensation water

Rainwater was collected at the Nerja Cave weather station (169 m a. s.l.). In general, the isotopic and chemical study was performed using the samples obtained during the main rainy periods, although sampling had been irregular during the study period.

Two types of condensation water were collected: (1) natural condensation water (Nw), that is, water directly visible on the ceiling and walls of the cave (in the form of individual drops) and (2) induced condensation water (Iw), sampled in areas C2, C3 and C4 (Figure 1). Nw has only been sampled in C2, the only accessible area with enough water to perform its subsequent chemical and isotopic analysis.

Natural condensation water was sampled “drop by drop,” avoiding areas where the rock substrate showed signs of alteration and in order to minimize “contamination” of the sample with secondary mineral components (Figure 2(a, b)). Although most of the drip points are linked to stalactites and soda straws stalactites, any drop of “doubtful” appearance on the walls has been also avoided in the sampling to minimize any possible mixing with infiltration waters. The quantity of sample that can be obtained with this method is normally very small (about 40 ml or less), limiting the analytical possibilities at the laboratory. The relatively small number of samples available is related to this circumstance as well as to the seasonal disappearance of natural condensation water during approximately 6 months per



FIGURE 2 (a) Sampling of natural condensation water (Nw) in the ceiling of the area C2. (b) Detailed photo of the sampling method. (c) Device for sampling induced condensation water (Iw) in the area C3 and (d) detailed photo of water condensed on the ice bag

year. The minimum exposure time of the natural condensation water with the cave atmosphere before the sampling was 7 days, considering the minimum time elapsed between two consecutive samplings. Collection of each sample took approximately 2 h.

To induce the condensation of air vapour of the cave atmosphere, plastic clean bags filled with ice were placed in the control areas (C2, C3 and C4 in Figure 1(a)). The bags were suspended so that the condensed water on its surface flowed downward to a sampling vessel (Figure 2(c, d)). The average time elapsed since the ice was placed inside the cave until the collection of the sample was 15 days.

From August 2013 to July 2015, the sampling period of both types of condensation water (Iw and Nw) was equivalent, except during periods in which Nw was absent in the cave (from mid-November 2014 to April 2015).

The pH and the electrical conductivity (EC) of the water were measured in situ, using HORIBA portable equipment, which allowed taking measurements with a minimum sample volume (several drops). pH was measured using the LAQUAtwin-pH -11 model pH meter (resolution: 0.1 pH, accuracy: ± 0.1 pH); EC was measured with the

LAQUAtwin-B771 model EC meter (resolution: $1 \mu\text{S}/\text{cm}$ for conductivity range 9–2000 $\mu\text{S}/\text{cm}$, accuracy $\pm 2\%$). Major inorganic ions and the isotopic composition of the water ($\delta^{18}\text{O}$ and $\delta^2\text{H}$) were analysed at the laboratory of the Centre of Hydrogeology of University of Malaga using a HPLC Ion Chromatography (METROHM mods. 881 Compact IC pro y 792 Basic IC) and a PICARRO water isotope analyser mods. L2120i. Raw isotope data referred to the Vienna-Standard Mean Ocean Water (VSMOW) and the accuracy of isotope measurements was $\pm 0.1 \%$ for $\delta^{18}\text{O}$ and $\pm 1.0 \%$ for $\delta^2\text{H}$. Saturation indices (calcite, dolomite) and the partial pressure of CO_2 in equilibrium with the solution—expressed as (PCO_2)— were calculated using the geochemical modelling software EQ3/6, version 8.0a (Wolery, 2013).

3.2 | Mineralogical and microbiological analysis

Two samples of the rock substrate (bedrock and moonmilk-type deposits) were collected in area C2 to characterize its mineralogical

composition. The mineralogical analyses were performed at the Central Research Support Services (SCAI) of the University of Malaga, using an X-ray diffractometer model PANalytical X'Pert PRO MRD. The *High Score Plus* software from PANalytical and the database *Powder Diffraction File* (PDF) were used to identify phases.

A sample with the appearance of a biofilm was also collected in the ceiling of control area C2 (Figure 1 (a)) by scalpel scraping under sterile conditions to determine its microbial community and its possible role or relationship with the chemical composition of the natural condensation water. The microbiological study, based on molecular analysis, was performed at the Institute of Natural Resources and Agrobiology of Seville, Spain (Jurado et al., 2018).

3.3 | Image analysis

From June 2017 to January 2018 the biweekly or monthly photo monitoring of a differentiated sub-area in control area C2 was carried out to document changes of the surface occupied by natural condensation water. The photos were taken with a digital camera *Canon PowerShot SX510 HS* with optical zoom $\times 30$, wide angle 24 mm, CMOS sensor with 12.1 megapixels and DIGIC 4, in order to obtain optimal results under low lighting conditions. A tripod located at a fixed point marked on the floor of the cave was used during the photo shoot in order to use the same location and orientation of the camera. Two images were obtained in each photo. In one of them, a scale was used to allow calibration of the images.

Digital photo analysis was performed using FIJI® software version 1.53c (Ferreira & Rasband, 2012). Firstly, the analysis area is manually selected on the original photograph with the Polygon Selection tool, establishing particularly significant elements of the image (spots, highlights, etc.) as vertices thereof; next, the program measures the surface of the selected area. After converting this clipping to 8-bit grayscale, it is segmented using lower and upper threshold values to differentiate the objects of interest (condensation water in our case) from the background with the greatest precision and objectivity. We applied the maximum threshold (255) as a constant value whilst the minimum value was established by the researcher in order to discriminate the area of interest from the images, that is, the presence of condensation water. After segmentation, we obtain a binary image (areas of condensation and non-condensation). Over this binary image, the surface occupied by the condensation water is determined in cm^2 . This process was repeated up to 10 times using the same thresholds in order to reduce possible human error, the final values being the average of the results obtained in each iteration.

4 | RESULTS

4.1 | Isotopic composition

Table 1 shows the results of the isotopic composition obtained from the samples analysed. In the rainwater, $\delta^{18}\text{O}$ ranged from -7.9

to -0.4 ‰, with a mean value of -4.0 ‰, while $\delta^2\text{H}$ ranged from -52.9 to -10.2 ‰, with a mean value of -24.4 ‰. In the natural condensation water (blue circles, Figure 3), $\delta^{18}\text{O}$ values ranged between -4.2 and -2.7 ‰, with a mean value of -3.2 ‰, while

TABLE 1 Isotopic data of the rainwater (Rw) and of the induced (Iw) and natural (Nw) condensation water in Nerja Cave for the period 2013–2018

| Area | Date | Rw | |
|------|-------------------|-----------------------|--------------------|
| | | $\delta^{18}\text{O}$ | $\delta^2\text{H}$ |
| WS | 6 September 2013 | -4.8 | -26.4 |
| | 2 October 2013 | -3.0 | -29.3 |
| | 22 October 2013 | -4.3 | -27.2 |
| | 22 September 2014 | -0.4 | -10.2 |
| | 29 September 2014 | -4.5 | -21.4 |
| | 14 October 2014 | -4.6 | -23.5 |
| | 4 November 2014 | -3.1 | -12.2 |
| | 9 November 2014 | -1.2 | -11.0 |
| | 13 November 2014 | -3.4 | -14.5 |
| | 28 November 2014 | -7.9 | -52.9 |
| | 19 October 2017 | -6.4 | -40.2 |
| | <i>n</i> | 11 | 11 |
| | max | -0.4 | -10.2 |
| | min | -7.9 | -52.9 |
| | mean | -4.0 | -24.4 |
| | <i>s</i> | 2.1 | 13.2 |
| | <i>v</i> (%) | -53.7 | -53.9 |
| Area | Date | Nw | |
| | | $\delta^{18}\text{O}$ | $\delta^2\text{H}$ |
| C2 | 5 September 2013 | -8.8 | -33.5 |
| | 19 September 2013 | -8.5 | -33.9 |
| | 30 October 2014 | -3.3 | -12.5 |
| | 5 November 2014 | -6.7 | -25.4 |
| | 14 November 2014 | -3.7 | -9.5 |
| | 20 November 2014 | -3.8 | -6.6 |
| | 11 December 2014 | -2.4 | 1.3 |
| C3 | 5 September 2013 | -9.5 | -38.8 |
| | 23 October 2013 | -5.4 | -25.9 |
| | 5 November 2014 | -3.7 | -11.9 |
| | 14 November 2014 | -3.9 | -7.1 |
| | 20 November 2014 | -0.8 | 8.8 |
| | 11 December 2014 | 0.3 | 16.4 |
| | | <i>n</i> | 13 |
| | max | 0.3 | 16.4 |
| | min | -9.5 | -38.8 |
| | mean | -4.6 | -13.7 |
| | <i>s</i> | 3.0 | 17.0 |
| | <i>v</i> (%) | -65.4 | 123.8 |

TABLE 1 (Continued)

| Area | Date | Nw | |
|--------------|-------------------|-----------------------|--------------------|
| | | $\delta^{18}\text{O}$ | $\delta^2\text{H}$ |
| C2 | 21 August 2013 | -3.2 | -12.5 |
| | 5 September 2013 | -4.2 | -20.5 |
| | 30 October 2014 | -3.2 | -12.5 |
| | 7 August 2017 | -2.7 | -11.5 |
| | 28 August 2017 | -3.0 | -13.5 |
| | 19 September 2017 | -3.4 | -14.5 |
| | 13 October 2017 | -3.1 | -14.6 |
| | 17 August 2018 | -3.6 | -17.8 |
| | 2 November 2018 | -2.8 | -8.1 |
| | <i>n</i> | | 9 |
| max | | -2.7 | -8.1 |
| min | | -4.2 | -20.5 |
| mean | | -3.2 | -13.9 |
| <i>s</i> | | 0.5 | 3.6 |
| <i>v</i> (%) | | 14.0 | -25.7 |

Note: They are expressed in ‰ and referred to the Vienna-Standard Mean Ocean Water (VSMOW). WS: weather station.

$\delta^2\text{H}$ content ranged from -20.5 to -8.1 ‰, with a mean value of -13.9 ‰. $\delta^{18}\text{O}$ of the induced condensation water (red circles, Figure 3) ranged from -9.5 to 0.3 ‰, with a mean value of -4.6 ‰,

while $\delta^2\text{H}$ ranged from -38.8 to 16.4 ‰, with a mean value of -13.7 ‰.

4.2 | Hydrochemistry, mineralogy and microbiology

The physico-chemical data of condensation water samples collected in Nerja Cave are presented in Tables 2 and 3 (induced and natural condensation water, respectively). The induced condensation water has a low mineralization, with electrical conductivity values (EC) between 32 and 273 $\mu\text{S}/\text{cm}$, and an average value of 116 $\mu\text{S}/\text{cm}$. They have PO_4^{3-} , F^- , K^+ and TOC (Total Organic Carbon) mean contents lower than 1 mg/L; Cl^- , Mg^{2+} and Na^+ contents of about 2–3 mg/L and NO_3^- and SO_4^{2-} contents of about 4–5 mg/L. The Ca^{2+} and HCO_3^- content are somewhat higher, 19 and 29 mg/L, respectively. The saturation indices show that these waters are undersaturated with respect to calcite (SI Cal = -1.31) and dolomite (SI Dol = -2.03). Iw samples present PCO_2 values ($\text{PCO}_{2[\text{Iw}]}$) that ranged from $10^{-3.71}$ to $10^{-3.23}$ atm, with a mean value of $10^{-3.37}$ atm (427 ppmv), lower than the cave air PCO_2 ($\text{PCO}_{2[\text{air}]}$) values measured during the sampling days, which ranged from $10^{-3.07}$ to $10^{-3.03}$ atm, with a mean value of $10^{-3.06}$ atm (871 ppmv).

The natural condensed water has higher mineralization, with EC values ranging between 209 and 720 $\mu\text{S}/\text{cm}$, and a mean value of 344 $\mu\text{S}/\text{cm}$. They have PO_4^{3-} , F^- , and TOC mean concentrations lower than 1 mg/L; Cl^- , Na^+ and SO_4^{2-} mean contents of about

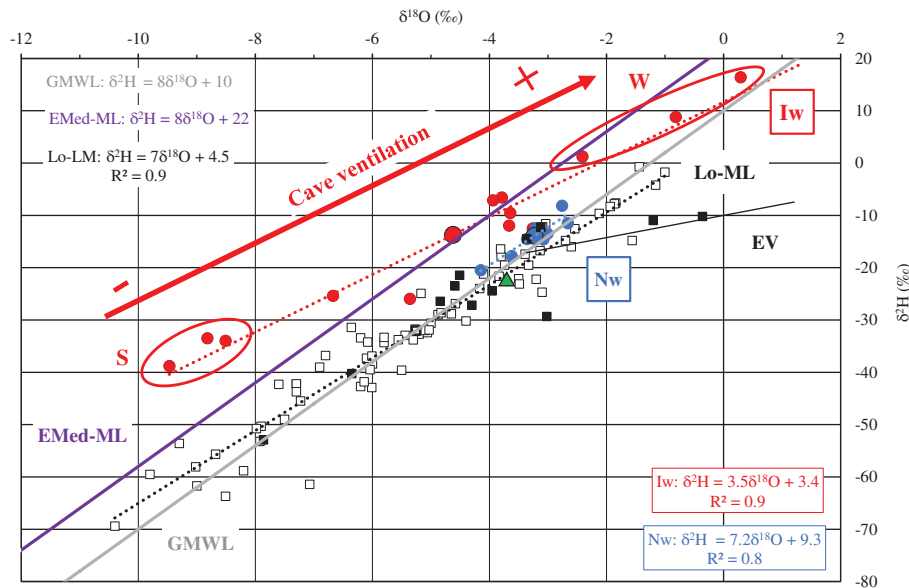


FIGURE 3 $\delta^{18}\text{O}$ - $\delta^2\text{H}$ plot of rainwater (squares) and condensation water (circles) obtained from the Nerja Cave and from the weather station. GMWL: Global meteoric water line, Lo-ML: Local meteoric water line, EMed-ML: Eastern Mediterranean meteoric water line, Nw: Condensation line for natural condensation water, Iw: Condensation line for induced condensation water, EV: Evaporation line, S: Summer samples, W: Winter/autumn samples. The largest circles/squares show the mean isotopic values for the different types of water. All the available isotopic data of the rainwater have been plotted on the graph: Black squares (period 2013–2017), white squares (1995–1999). The green triangle shows the mean isotopic value for the drip water ($\delta^{18}\text{O}$: -3.8‰, $\delta^2\text{H}$: -22.1‰) according to Carrasco et al. (2006)

TABLE 2 Physico-chemical data of induced condensation water in Nerja Cave

| Area | Date | pH | EC | HCO ₃ ⁻ | Ca ²⁺ | Mg ²⁺ | Na ⁺ | K ⁺ | Cl ⁻ | NO ₃ ⁻ | SO ₄ ²⁻ | PO ₄ ³⁻ | F ⁻ | TOC | SI Cal | SI Dol | PCO ₂ |
|------------------|-------------------|------|-----|-------------------------------|------------------|------------------|-----------------|----------------|-----------------|------------------------------|-------------------------------|-------------------------------|----------------|------|--------|--------|------------------|
| C2 | 25 July 2013 | | 51 | | | | | | | | | | | | | | |
| | 21 August 2013 | 7.30 | 57 | | | | | | | | | | | | | | |
| | 29 August 2013 | 7.80 | 61 | | | | | | | | | | | | | | |
| | 5 September 2013 | 7.50 | 75 | 18.00 | 7.60 | 0.90 | 1.80 | 0.30 | 1.30 | 1.80 | 6.30 | | | 0.60 | -1.79 | -3.14 | -3.30 |
| | 19 September 2013 | 7.60 | 32 | 25.00 | 7.60 | 1.60 | 1.20 | 0.40 | 1.40 | 3.30 | 4.80 | | | | -1.54 | -2.39 | -3.25 |
| | 1 October 2013 | 8.00 | 143 | | | | | | | | | | | | | | |
| | 30 October 2014 | 8.00 | 260 | | | | | | | | | | | | | | |
| | 5 November 2014 | 8.10 | 76 | | 14.67 | 1.97 | 1.98 | 0.20 | 1.46 | 1.62 | 1.62 | 4.75 | 0.09 | | | | |
| | 14 November 2014 | 7.90 | 95 | | 20.20 | 2.23 | 2.58 | 0.63 | 2.04 | 0.81 | 5.09 | 0.18 | 0.04 | | | | |
| | 20 November 2014 | 8.10 | 127 | | 25.52 | 1.55 | 4.83 | 1.85 | 5.37 | 2.80 | 6.02 | | 0.04 | | | | |
| | 11 December 2014 | 8.10 | 123 | | 27.98 | 0.97 | 2.78 | 1.22 | 2.87 | 2.82 | 5.14 | | 0.04 | | | | |
| | 20 January 2015 | 8.26 | 160 | | | | | | | | | | | | | | |
| | 20 March 2015 | 8.40 | 240 | | | | | | | | | | | | | | |
| | 20 April 2015 | | | | 21.55 | | 7.89 | 0.65 | 1.94 | 2.47 | 5.02 | | 0.04 | | | | |
| | 25 June 2015 | 7.75 | 117 | | 30.92 | 0.94 | 2.33 | 1.44 | 2.69 | 5.23 | 5.18 | | | | | | |
| | 6 July 2015 | 7.44 | 120 | | 27.85 | 1.01 | 2.72 | 1.30 | 3.01 | 6.66 | 5.33 | | | | | | |
| | 24 July 2015 | 7.90 | 144 | | | | | | | | | | | | | | |
| | 6 August 2015 | 7.55 | 123 | | | | | | | | | | | | | | |
| | 14 August 2015 | 7.70 | 273 | | | | | | | | | | | | | | |
| | 17 September 2015 | 7.70 | 190 | | | | | | | | | | | | | | |
| 22 October 2015 | 7.50 | 197 | | | | | | | | | | | | | | | |
| 29 June 2017 | 7.50 | 71 | | | | | | | | | | | | | | | |
| 3 August 2017 | 6.80 | 112 | | | | | | | | | | | | | | | |
| C3 | 23 August 2013 | 8.00 | 87 | | | | | | | | | | | | | | |
| | 5 September 2013 | 7.90 | 55 | 51.00 | 12.00 | 4.40 | 2.20 | 0.70 | 2.40 | 5.30 | 5.10 | | | 0.43 | -0.75 | -0.57 | -3.23 |
| | 19 September 2013 | 7.90 | 82 | | | | | | | | | | | | | | |
| | 1 October 2013 | 7.90 | 45 | | | | | | | | | | | | | | |
| | 23 October 2013 | 8.00 | 42 | 21.00 | 8.50 | 0.70 | 1.30 | 0.60 | 1.40 | 3.30 | 4.70 | 0.15 | 0.04 | 0.55 | -1.16 | -2.02 | -3.71 |
| | 14 November 2014 | 7.80 | 57 | | 6.67 | 2.69 | 2.59 | 0.33 | 2.13 | 6.69 | 5.02 | | | | | | |
| 20 November 2014 | 7.90 | 102 | | | | | | | | | | | | | | | |
| 11 December 2014 | 8.20 | 131 | | 19.33 | 4.25 | 2.43 | 1.50 | 2.48 | 7.88 | 5.39 | 0.29 | 0.04 | | | | | |
| 20 March 2015 | 8.00 | 144 | | 34.85 | 0.80 | 0.64 | 0.53 | 1.43 | 0.88 | 5.21 | | 0.05 | | | | | |

TABLE 2 (Continued)

| | | | | | | | | | | | | | | | | | | | |
|-------|------|-----|-------|-------|-------|-------|-------|-------|-------|------|-------|-------|-------|--------|-------|-------|--------|--------|-------|
| n | 30 | 31 | 4 | 14 | 13 | 14 | 14 | 14 | 14 | 14 | 14 | 14 | 14 | 4 | 7 | 3 | 4 | 4 | 4 |
| max | 8.40 | 273 | 51.00 | 34.85 | 4.40 | 7.89 | 1.85 | 5.37 | 7.88 | 6.30 | 0.29 | 0.05 | 0.60 | -0.75 | 0.60 | 0.43 | -0.57 | -3.23 | -3.23 |
| min | 6.80 | 32 | 18.00 | 6.67 | 0.70 | 0.64 | 0.20 | 1.30 | 0.81 | 4.70 | 0.09 | 0.04 | 0.43 | -1.79 | 0.43 | 0.53 | -3.14 | -3.71 | -3.71 |
| mean | 7.82 | 116 | 28.75 | 18.95 | 1.85 | 2.66 | 0.83 | 2.28 | 3.68 | 5.22 | 0.18 | 0.04 | 0.53 | -1.31 | 0.04 | 0.09 | -2.03 | -3.37 | -3.37 |
| s | 0.32 | 63 | 15.11 | 9.58 | 1.26 | 1.79 | 0.52 | 1.07 | 2.28 | 0.45 | 0.08 | 0.01 | 0.45 | 0.45 | 0.09 | 0.45 | 1.08 | 1.08 | 0.23 |
| v (%) | 4.13 | 55 | 52.55 | 50.55 | 68.00 | 67.33 | 63.00 | 46.74 | 61.96 | 8.62 | 46.01 | 13.87 | 16.59 | -34.69 | 16.59 | 16.59 | -53.16 | -53.16 | -6.73 |

Note: Ion contents and TOC are expressed in mg/L.

Abbreviations: EC, Electrical conductivity (in $\mu\text{S}/\text{cm}$); max, Maximum value; min, Minimum value; n, Number of samples; PCO_2 , Partial pressure of CO_2 in equilibrium with the solution, expressed as $-\log \text{PCO}_2$; s, Standard deviation; SI Cal, Calcite saturation index; SI Dol, Dolomite saturation index; TOC, Total organic carbon; v, Variation coefficient.

8–10 mg/L; Ca^{2+} and Mg^{2+} mean contents of about 25 mg/L and an average value of HCO_3^- of about 150 mg/L. In most samples, the NO_3^- content is remarkably high, between 30 and 130 mg/L, with an average value of 45.5 mg/L. Only in two samples the nitrate concentration was 5.0 mg/L. The saturation indices show that these waters are slightly undersaturated with respect to calcite (SI Cal = -0.29) and supersaturated in dolomite (SI Dol = 0.59). Nw samples present PCO_2 values that ranged from $10^{-3.21}$ to $10^{-2.08}$ atm, with a mean value of $10^{-2.53}$ atm (2951 ppmv). These values are much higher than the measured cave air PCO_2 , ranging from $10^{-3.19}$ to $10^{-3.06}$ atm, with a mean value of $10^{-3.15}$ atm (708 ppmv).

The mineralogical analyses performed in area C2 (Figure 4) indicated that, in the bedrock sample, dolomite was identified as the main crystalline phase and also hydromagnesite, although in very low proportion. In the moonmilk-type deposits, hydromagnesite was identified as the only crystalline phase.

The microbiological analysis of the substrate sample of biofilm appearance collected in area C2 (see Figure 4) showed a distinctive microbial community compared to the usual microorganisms inhabiting the cave, characterized by the greatest abundance of *Gammaproteobacteria* (*Nitrosococcaceae* family) (Jurado et al., 2018).

4.3 | Image analysis

The data obtained after the image analysis performed in area C2 are presented in Table 4. The Total area is the total surface of the selected clipping in the image (yellow polygon in Figure 5). Water area corresponds to the surface occupied by the condensation water in this clipping, expressed in cm^2 and percentage of surface (%) with respect to the Total area. The obtained results show that the surface occupied by the condensation water in the control area has varied during the studied period (Figure 5), allowing us to quantify such variation.

The percentage of rock substrate covered by condensation water increased from 0.03% in June until reaching a maximum value in August, when 0.51% of the surface analysed was covered by condensation water. From August until November, the surface occupied by condensation water decreased until reaching 0.30% in November, and disappeared in December and January (0% of surface covered by condensation water).

5 | DISCUSSION

5.1 | Isotopic composition

By plotting the isotopic data on a $\delta^{18}\text{O}$ - $\delta^2\text{H}$ chart (Figure 3), we observe that rainwater samples are aligned according to the Global meteoric water line (GMWL, grey line in Figure 3) established by Craig (1961) and the local meteoric water (Lo-ML, dotted black line in Figure 3). Some evaporated samples are also observed in Figure 3 (Ev, black line). The rainwater samples lie between the Eastern

TABLE 3 Physico-chemical data of natural condensation water in Nerja Cave sampled in area C2

| Date | pH | EC | HCO ₃ ⁻ | Ca ²⁺ | Mg ²⁺ | Na ⁺ | K ⁺ | Cl ⁻ | NO ₃ ⁻ | SO ₄ ²⁻ | PO ₄ ³⁻ | F ⁻ | TOC | SI Cal | SI Dol | PCO ₂ |
|-------------------|------|-----|-------------------------------|------------------|------------------|-----------------|----------------|-----------------|------------------------------|-------------------------------|-------------------------------|----------------|-------|--------|--------|------------------|
| 21 August 2013 | 8.00 | | | 20.18 | 31.52 | 9.18 | 0.53 | 12.43 | 41.07 | 13.56 | 0.15 | 0.10 | | | | |
| 22 August 2013 | 8.30 | | | | | | | | | | | | | | | |
| 29 August 2013 | 8.20 | 300 | | | | | | | | | | | | | | |
| 5 September 2013 | 8.20 | 320 | 112.00 | 22.30 | 23.10 | 8.80 | 1.10 | 14.10 | 32.40 | 20.50 | 0.15 | 0.10 | 0.79 | 0.09 | 1.56 | -3.21 |
| 19 September 2013 | 8.00 | | | | | | | | | | | | | | | |
| 1 October 2013 | 8.30 | 480 | | | | | | | | | | | | | | |
| 30 October 2014 | 8.00 | 283 | | 20.18 | 31.52 | 9.18 | 0.53 | 12.43 | 41.07 | 13.56 | 0.15 | 0.10 | | | | |
| 5 November 2014 | 8.10 | 220 | | | | | | | | | | | | | | |
| 14 November 2014 | 8.00 | 250 | | | | | | | | | | | | | | |
| 29 June 2015 | | | | 32.73 | 51.21 | 10.37 | 1.05 | 6.16 | 31.98 | 9.37 | 0.25 | 0.12 | | | | |
| 24 July 2015 | 7.70 | 325 | | | | | | | | | | | | | | |
| 6 August 2015 | 7.78 | 209 | | 17.73 | 23.36 | 6.30 | 0.48 | 7.43 | 30.76 | 9.28 | | 0.09 | | | | |
| 14 August 2015 | 7.70 | 320 | | 19.25 | 25.40 | 5.59 | 0.58 | 7.03 | 40.80 | 9.74 | | 0.10 | | | | |
| 28 August 2015 | 7.85 | 259 | | 18.47 | 26.72 | 4.87 | 0.46 | 5.23 | 34.34 | 8.56 | | 0.10 | | | | |
| 17 September 2015 | 7.70 | 299 | | | | | | | | | | | | | | |
| 22 October 2015 | 7.70 | 243 | | | | | | | | | | | | | | |
| 22 July 2016 | 7.70 | 355 | | 21.36 | 35.89 | 7.45 | 0.75 | 12.88 | 80.60 | 8.74 | | 0.05 | | | | |
| 29 July 2016 | 7.80 | 325 | | 23.53 | 44.02 | 9.59 | 0.67 | 14.64 | 130.07 | 8.15 | | 0.10 | | | | |
| 5 August 2016 | 7.70 | 300 | | 17.41 | 31.83 | 8.39 | 0.49 | 7.29 | 65.50 | 6.59 | | 0.11 | | | | |
| 28 June 2017 | 7.20 | 720 | | | | | | | | | | | | | | |
| 3 August 2017 | 7.00 | 440 | | | | | | | | | | | | | | |
| 7 August 2017 | 7.15 | | 146.16 | 38.50 | 3.90 | 9.60 | 4.00 | 4.80 | 5.10 | 3.10 | | 0.10 | -0.63 | -0.88 | | -2.08 |
| 28 August 2017 | 7.40 | 280 | 143.47 | 37.20 | 10.00 | 8.30 | 2.10 | 1.60 | 5.40 | 3.00 | | | -0.39 | 0.04 | | -2.32 |
| 19 September 2017 | 7.30 | 480 | 180.56 | 34.70 | 33.40 | 12.30 | 17.40 | 36.80 | 106.50 | 20.00 | | 0.30 | -0.47 | 0.42 | | -2.14 |
| 13 October 2017 | 6.80 | 410 | | 26.10 | 12.00 | 5.40 | 1.20 | 10.80 | 35.80 | 18.80 | | | | | | |
| 6 July 2018 | | 430 | | | | | | | | | | | | | | |
| 17 August 2018 | 7.79 | | 150.00 | 20.00 | 31.30 | | | 4.30 | 29.00 | 7.20 | | 0.10 | -0.25 | 1.08 | | -2.67 |
| 10 September 2018 | 7.86 | 320 | 150.00 | 25.00 | 33.50 | | | 1.40 | 33.50 | 8.30 | | 0.20 | -0.09 | 1.34 | | -2.74 |
| 2 November 2018 | | | | 17.20 | 23.00 | 5.80 | 0.20 | 5.70 | 30.00 | 4.00 | | 0.10 | | | | |

TABLE 3 (Continued)

| | | | | | | | | | | | | | | | | | |
|-------|------|-----|--------|-------|-------|-------|-------|-------|--------|-------|-------|-------|-------|--------|--------|--------|-------|
| n | 26 | 22 | 6 | 17 | 17 | 15 | 15 | 17 | 17 | 17 | 17 | 3 | 14 | 1 | 6 | 6 | 6 |
| max | 8.30 | 720 | 180.56 | 38.50 | 51.21 | 12.30 | 4.87 | 36.80 | 130.07 | 20.50 | 0.25 | 0.30 | 0.09 | 0.79 | 0.79 | 1.56 | -2.08 |
| min | 6.80 | 209 | 112.00 | 17.20 | 3.90 | 8.07 | 4.87 | 1.40 | 5.10 | 3.00 | 0.15 | 0.05 | 0.05 | 0.79 | 0.79 | -0.63 | -3.21 |
| mean | 7.74 | 344 | 147.03 | 24.23 | 27.74 | 8.07 | 8.07 | 9.71 | 45.52 | 10.14 | 0.18 | 0.12 | 0.12 | 0.79 | 0.79 | -0.29 | -2.53 |
| s | 0.39 | 115 | 21.83 | 7.15 | 11.74 | 2.12 | 2.12 | 8.13 | 32.84 | 5.45 | 0.06 | 0.06 | 0.06 | 0.26 | 0.26 | 0.92 | 0.43 |
| v (%) | 5.09 | 33 | 14.85 | 29.50 | 42.32 | 26.30 | 26.30 | 83.80 | 72.14 | 53.76 | 30.62 | 51.29 | 51.29 | -90.45 | 155.39 | -17.02 | |

Note: Ion contents and TOC are expressed in mg/L.

Abbreviations: EC, Electrical conductivity (in $\mu\text{S}/\text{cm}$); max, Maximum value; min, Minimum value; n, Number of samples; PCO_2 , Partial pressure of CO_2 in equilibrium with the solution, expressed as $-\log \text{PCO}_2$; s, Standard deviation; SI Cal, Calcite saturation index; SI Dol, Dolomite saturation index; TOC, Total organic carbon; v, Variation coefficient.

Mediterranean meteoric water line (EMed-ML, purple line in Figure 3) (Gat & Garmi, 1987) and the GMWL, showing the Atlantic and Mediterranean origin of the rainfalls in the region. The isotopic composition (Table 1) is similar to those reported by Carrasco et al. (2006) in 79 rainwater samples collected during the period 1995–1999 (white squares in Figure 3). However, our results (black squares in Figure 3) show more negative maximum values of $\delta^{18}\text{O}/\delta^2\text{H}$ ($-0.4\text{‰}/-10.2\text{‰}$) than those reported by Carrasco et al. (2006) ($1.2\text{‰}/13.7\text{‰}$) because all the rainwater samples in our study were collected in autumn/winter. During the summer, the rainwater of Nerja has more enriched values of $\delta^{18}\text{O}$ and $\delta^2\text{H}$: rainwater drops tend to evaporate during their descent through a very dry atmosphere, which also carries an enrichment of the isotopic content, depending on the amount effect and on the seasonal effect (Carrasco et al., 2006).

The condensation water samples fit on two condensation lines, with a slope of 3.5 (lw, red dotted line in Figure 3) and 7.2 (Nw, blue dotted line). Due to the large temperature difference between the cave air and the ice bag surface used for sampling, isotopic fractionation may occur, with preferential condensation of the heavy isotopes. Thus, the theoretical isotopic composition of the cave air vapour water would lie over the lw line, towards the more negative values, as long as there is no isotopic exchange with the cave atmosphere.

The isotopic composition of Nw is more homogeneous than that lw and similar to those of drip waters (green triangle). This could be a hint for that the vapour water condensing on the cave originates, in part, from the evaporation of dripping and splashing waters. These waters would evaporate, be transported to other cave locations, and lastly condense (Dublyansky & Dublyansky, 1998) under stable conditions of temperature and humidity, without external factors disturbing the equilibrium.

The isotopic composition of the lw samples show a different seasonal variation than those of rainwater, with more negative $\delta^{18}\text{O}$ and $\delta^2\text{H}$ values during the summer (September, group S in Figure 3), more positive values around the winter (end of November and December, group W in Figure 3) and intermediate values during the autumn (rest of samples in Figure 3). Winter is the period of the year in which the natural ventilation of the cave is at a maximum (Dueñas et al., 2011) and the relative humidity of the air of the Tourist Galleries is lower (60%–80%). Thus, less negative $\delta^{18}\text{O}$ - $\delta^2\text{H}$ values would indicate evaporation processes of the condensed water drops (in contact with the cave atmosphere) before the sampling. Conversely, during the summer, the natural ventilation of the cave is minimum and the relative humidity of the air is higher (98%–100%). Thus, evaporation of the condensed water drops would be minimum and no enrichment of the isotopic composition would be produced. lw line, with a slope of 3.5, is a clear indication of an evaporation process of cave water vapour during winter. This evaporative process is not caused by temperature because inside the cave, and especially in the area where samples were taken, the temperature variation is very low. Therefore, the renovation of air masses during winter seems to be the factor driving the enrichment of water vapour inside the cave.

The isotopic values of the Nw samples are always negative (Table 1). The samples were collected in summer and autumn, when the evaporation processes inside the cave are minimum or lower than during the winter. In winter, coinciding with the switch to *winter* mode ventilation in the cave (Liñán et al., 2018, 2020), the natural condensation water in sectors C2 and C3 disappears.

5.2 | Hydrochemistry, mineralogy and microbiology

The induced condensation water (lw) is considered as the “input signal” in the cave system, and its physico-chemical characteristics will be more or less modified when it comes into contact with the bedrock and/or the speleothems of the cave, although possible interference with secondary minerals or biofilms must also be considered. The comparison of the physico-chemical characteristics of lw with those of the natural condensation water (Nw) or “output signal” will allow us to identify the processes that occur on the solid substrate.

The first aspect that stands out is that the lw samples are not in chemical equilibrium with the cave air PCO_2 . As the solution was collected relatively fast in the flask located below the ice bag, a possible explanation for this “disequilibrium” between cave air PCO_2 and water PCO_2 could be that, in the flask, the surface to volume ratio is comparably high and diffusion takes more time into the solution compared to a thin solution film on the cave wall. However, the average time elapsed since the ice was placed inside the cave until the sampling collection was 15 days, a relatively long time for the chemical equilibrium to be established.

Cardenal et al. (1999) showed that the pH of the cave drip water samples increased (up to 0.6 points) as the contact time between the drip water sample and the cave atmosphere increased, as a result of the degasification processes in the water sample previous to the pH

measurement. Afterward (18 samples collected in 2019), we have measured pH increases (up to 0.8 points) between the pH measured directly in the drip water points (before the water falls) and the pH of the water collected after a week in the flask located below them. The same process must occur in the induced condensation water samples (lw). Their original pH values (before sampling) might be lower than those that we measured and used to calculate the $\text{PCO}_{2(w)}$, which would result in higher values of $\text{PCO}_{2(w)}$ compared to the $\text{PCO}_{2(\text{air})}$ values.

The saturation indices show that the lw waters are undersaturated with respect to calcite and dolomite so, in contact with a CO_2 -rich atmosphere, they are potentially aggressive; that is, they can dissolve the carbonate bedrock and speleothems with which they come into contact. Indeed, the higher HCO_3^- , Ca^{2+} and Mg^{2+} contents in the natural condensation water with respect to those of the induced condensation water evidence the existence of the “corrosion condensation” process: the undersaturated water comes into contact with the bedrock in a CO_2 -rich atmosphere, and the dissolution of the dolomitic/calcitic substrate (bedrock and speleothems) begins. At the moment of sampling, the condensation water had already dissolved the bedrock/speleothems and increased its mineralization and its bicarbonate, calcium and magnesium contents. As the kinetic of the dissolution of dolomite is slower than that of the calcite, it can be expected that the calcium contents increased more than the magnesium contents after the dissolution of the substrate. However, a much higher increase in the magnesium concentration is observed (from 1.9 mg/L in lw to 27.7 mg/L in Nw) than in that of calcium (from 19.0 mg/L in lw to 24.2 mg/L in Nw) (Table 5). This suggests that the substrate affected by the dissolution in area C2 is essentially of dolomitic nature. This agrees with the results obtained from the mineralogical analysis conducted in this sector of the cave as we indicate below. A fact to consider is that the Nw samples can actually be composite samples, that is, many drops from several

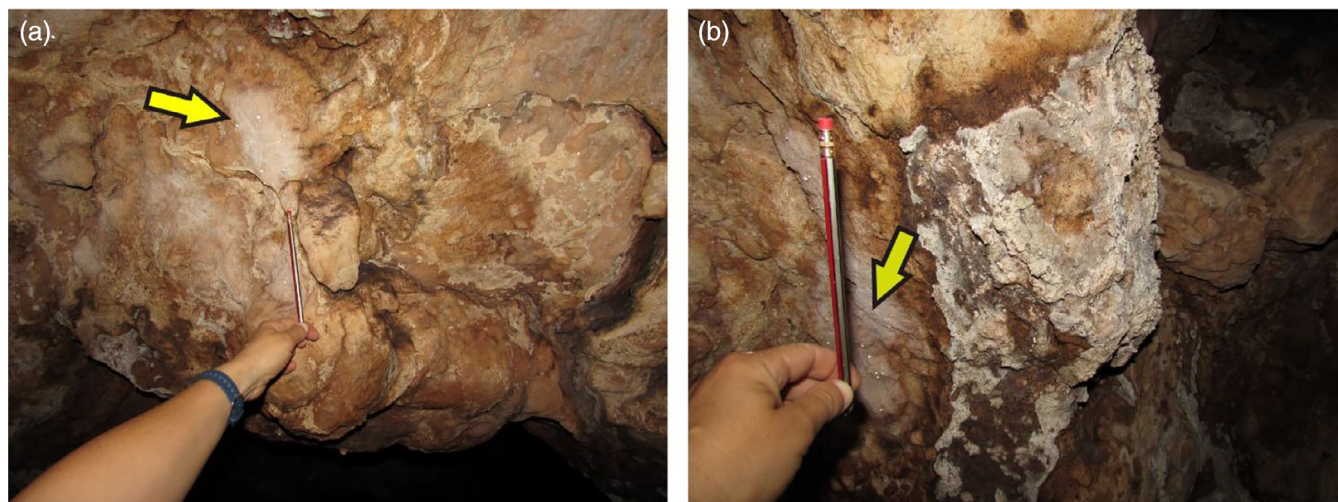


FIGURE 4 On the left, sampling area of the bedrock. On the right, sampling area of moonmilk-type deposits. Both areas are located in area C2 (chamber H-3). The white colour areas with biofilm appearance are also visible in the images (yellow arrows) and some bright drops of natural condensation water

TABLE 4 Results of image analysis

| Date | Total area (cm ²) | Water area (cm ²) | Water area (%) | Water area (% Rel.) | V (%) -Total area | V (%) -Water area |
|-------------------|-------------------------------|-------------------------------|----------------|---------------------|-------------------|-------------------|
| 21 June 2017 | 5608.09 | 01.55 | 0.03 | 5 | 0.18 | 0.28 |
| 07 August 2017 | | 23.65 | 0.42 | 83 | 0.16 | 0.06 |
| 28 August 2017 | | 28.49 | 0.51 | 100 | 0.17 | 0.03 |
| 19 September 2017 | | 22.08 | 0.39 | 77 | 0.15 | 0.06 |
| 13 October 2017 | | 17.35 | 0.31 | 61 | 0.14 | 0.05 |
| 10 November 2017 | | 17.05 | 0.30 | 60 | 0.24 | 0.32 |
| 18 December 2017 | | 04.49 | 0.00 | 1 | 0.27 | 1.57 |
| 31 January 2018 | | 00.19 | 0.00 | 1 | 0.26 | 2.75 |

Note: The surface occupied by condensation water is expressed in cm² (Water area (cm²)) and in percentage (Water area %) with respect to the total surface of the clipping or yellow polygon in Figure 5 (Total area (cm²)). Water area (% Rel.) represents the evolution (in %) of the surface occupied by condensation water (maximum value in August and minimum values in December and January). The table also includes the average variation coefficients of the Total area (cm²) and Water area (cm²), calculated for each group of 10 analysed images.

sectors located meters away become mixed, and so it is likely that we have sampled many drops located on hydromagnesite speleothems and few drops of water condensed on calcite speleothems or bedrock.

Due to the high difference between the PCO₂ of the natural condensation water in Nerja Cave and the cave atmosphere, CO₂ degasses from the solution by molecular diffusion. Dreybrodt and Scholz (2011) and Hansen et al. (2013) reported that the diffusion of CO₂ in thin films of water (as in the case of condensation water) is very fast. The dolomitic nature of the rock/speleothem limits the Ca²⁺ content of the dissolution and favours a high Mg²⁺/Ca²⁺ relation. So, rapid degassing of the drops of condensed water enriched with Mg²⁺ would cause the solution to become supersaturated with respect to the dolomite and, ultimately, dolomite and hydromagnesite may precipitate.

In Nerja Cave, the degassing of the condensed natural water (Nw) leaves carbonate deposits enriched with Mg²⁺ with whitish, flaky and unsightly appearance, similar to those reported by De Freitas and Schmekal (2003) in the Glowworm Cave (New Zealand). In the Castañar Cave (Spain), Alonso-Zarza and Martín Pérez (2008) reported that Mg-Ca carbonates are forming as the final products of precipitation from water that becomes relatively enriched with respect to Mg²⁺ due to the initial precipitation of aragonite and calcite. Casas et al. (2001) also detailed the depositional sequence for the carbonates of the moonmilk-type deposits in the Nerja Cave starting with initial precipitation of calcium carbonates, which removes Ca²⁺ from the cave water, increasing the Mg²⁺/Ca²⁺ relation. The rapid and progressive evaporation makes the water become increasingly enriched with Mg²⁺ and the degassing of the dissolved CO₂ would cause the precipitation of dolomite.

During the carbonate precipitation process, CO₂ is released into the solution. Laboratory experiments performed by Dreybrodt and Scholz (2011) showed that the slow degassing of physically dissolved CO₂ causes a slight supersaturation with respect to calcite, and calcite precipitates slowly. During precipitation of calcite, degassing of physically dissolved CO₂ and degassing of CO₂ originating from calcite

precipitation occur simultaneously. However, for thin water layers, degassing of physically dissolved CO₂ is driven by molecular diffusion, which is one order of magnitude faster than the subsequent calcite precipitation. Thus, the degassing occurs in two steps: (1) degassing of dissolved CO₂ and (2) degassing of the CO₂ resulting from calcite precipitation.

Our results seem to be in good agreement with the laboratory results of Dreybrodt and Scholz (2011). Inside the cave, the air CO₂ is dissolved in the natural condensation water in contact with the bedrock, and the substrate dissolution begins. The dissolution continues until the water becomes supersaturated and the carbonate minerals precipitate. During the carbonate precipitation process, CO₂ is released into the solution, increasing the PCO_{2(Nw)}. The CO₂ arising from the carbonate precipitation would degas slower than the dissolved CO₂. This would result in substantially higher PCO_{2(Nw)} values than PCO_{2 (air)}.

Cave air dynamics play a vital role in the seasonal variation in the carbonate system parameters (Spötl et al., 2005), modifying the PCO₂ gradient between the air and the cave waters. A high PCO₂ gradient between the cave air and the drip waters would enhance the CO₂ degassing and the concomitant carbonate deposition favouring the precipitation of CaCO₃ from the solution due to higher supersaturation. On the contrary, high PCO₂ levels inside the cave would reduce the thermodynamic drive for carbonate precipitation (lower driving force), eventually causing corrosion of the existing speleothem formations. Liñán et al. (2000) have also observed this relationship between cave air CO₂ content and the higher or lower precipitation of CaCO₃.

A seasonal variation in the air PCO₂ of the Tourist Galleries exists throughout the year. In the colder months, cave air PCO₂ presents low values (about 550 ppmv from November to March), maximum ventilation rate (Dueñas et al., 2011), lower number of visitors (12 000–30 000 people/month), and reduced drip water flow. During the warm months (from June to October), the air PCO₂ (>800 ppmv) and the number of visitors (between 35 000 and 79 000 people/month) are higher than in the colder months. In the warm season natural ventilation decreases, and there is a greater drip flow that

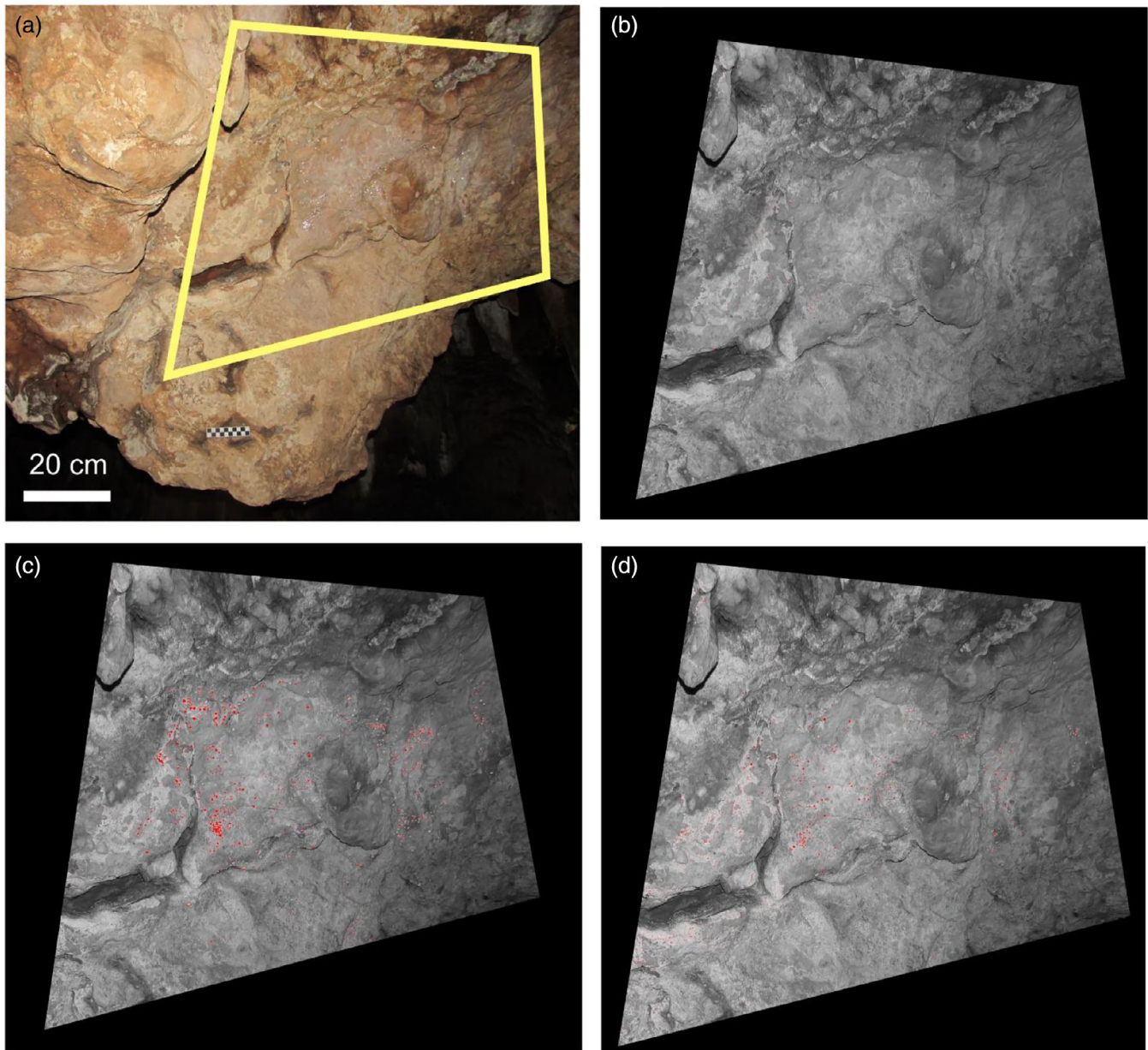


FIGURE 5 (a) Example of image taken in area C2. The yellow polygon delimits the sub-area (clipping) used to perform the image analysis. Scale is 10 cm length; (b–d) sub-areas after clipping and quantification of the pixels which correspond to the presence of condensation water (red colour). These images were taken on 21 June, 28 August and 10 November

introduces water rich in CO_2 from the soil. Benavente et al. (2010) have determined that the high Mg^{2+} content value of the cave drip water could only be produced by dolomite dissolution in an environment of very high PCO_2 , approximately 100 times greater than the external atmosphere. This value is similar to the average concentration of CO_2 recorded in the air of several research boreholes located northwest of the cave entrance. The condensation water is observed just in the warm season, coinciding with very high relative humidity values (98%) and high PCO_2 levels inside the cave, and thus, a higher aggressiveness (corrosion potential) than would exist if it were to condense during the cold season.

The natural condensation water shows unexpected relatively high nitrate concentrations. In the Nw they are 12 times greater (45.52 mg/L) than in the lw (3.68 mg/L). High nitrate concentrations were also detected in condensation water in the Altamira Cave (N of Spain), with values ranging between 17.8 and 38.0 mg/L and an average value of 26.82 mg/L in six samples collected in the period 2003–2005 (Cuezva, 2008). These nitrate concentrations are related to the development of some microbial communities underground, which can favour the biodeterioration processes associated with them. In the case of Altamira, corrective measures were implemented (reduction of vegetation cover in the area of direct infiltration,

including elimination of plant debris and control of plant growth) and the nitrate concentration in the drip waters was reduced down to average values lower than 10 mg/L in the period 2006–2009 (Sánchez-Moral et al., 2014).

In the surroundings of the Nerja Cave there are no industrial, agricultural or livestock activities or any significant vegetal cover that could be the source of the high nitrate contents found in the natural condensation water. Indeed, the average nitrate content in the drip waters of the cave is 5.45 mg/L (Andreo & Carrasco, 1993). The average nitrate content in the water of Maro spring, the main discharge point of the aquifer in the sector where the cave is located, was 0.4 mg/L for the period 1995–1998 and 1.0 mg/L for the period 2004–2013 (Vadillo et al., 2016). Thus, there is no external contamination by nitrates or a contribution of nitrate by mixing with drip waters that could relate to the source of nitrates in the condensation water. For this reason, the high nitrate values found in the natural condensation water seem to be associated with the rocky substratum where condensation is produced, and not with the drip waters, the activities or processes occurring outside the cave. There is also no presence of bat guano in the sampling area C2 or its surroundings.

Two hypotheses have been considered regarding the origin of nitrate content in the natural condensation water of Nerja Cave: (1) the presence in the bedrock and/or speleothems of some nitrate

minerals, such as nitrocalcite [$\text{Ca}(\text{NO}_3)_2 \cdot 4\text{H}_2\text{O}$] or nitromagnesite [$\text{Mg}(\text{NO}_3)_2 \cdot 6\text{H}_2\text{O}$], and (2) the existence of nitrifying bacteria in the bedrock and/or speleothems of the cave.

Hill and Buecher (1992) cite guano and limestone as a source of nitrate and calcium of the nitrocalcite found in Karchtner caverns (USA). Nitromagnesite has also been described as a product of the leaching of bat guano in Independence Cave (Botswana) (Hill & Forti, 1997) or in relation with olive orchards on the surface that supply nitrates to seeping groundwater in the Pulo di Molfetta caves (Forti & Palmisano, 1989). Martínez-Arkarazo et al. (2008) identified several nitrate minerals, including nitrocalcite, niter, gwihabait, nitromagnesite and nitratine, in moonmilk-type deposits sampled in Pozalagua Cave (N of Spain). They were related to shepherding activities on the surface.

So far, mainly carbonate minerals have been identified and described in the Nerja Cave as follows: aragonite, calcite and dolomite in the speleothems (Reyes et al., 1993), dolomite, hydromagnesite and mica in the bedrock (Reyes et al., 1993) and aragonite, calcite, dolomite, huntite, magnesite and hydromagnesite in moonmilk-type speleothems (Casas et al., 2001; Casas et al., 2002). The mineralogical analysis performed in this study shows that dolomite and hydromagnesite are the only crystalline phases identified in the bedrock and the moonmilk-type deposit samples taken in area C2 (Figure 4). Therefore, the presence of nitrate minerals in the rock substrate that could be dissolved by condensation water is discarded.

However, the results of the microbiological analysis performed in this area show a microbial community characterized by the greatest abundance of *Gammaproteobacteria* (*Nitrosococcaceae* family). The family *Nitrosococcaceae*, with the genus *Nitrosococcus*, plays a critical role in the global nitrogen cycle due to its capacity to oxidize ammonia (NH_4) to nitrite, the first step of nitrification (biological oxidation of ammonia to nitrite followed by oxidation of nitrite to nitrate). In the Nerja Cave, the non-cultivable genus *wb1-P19* (family *Nitrosococcaceae*) was found, the sequence of which is included by Holmes et al. (2001) among sulfur and nitrite oxidizing gammaproteobacteria. However, it cannot be concluded whether these Nerja sequences also have a role in nitrification, given the lack of data, but it seems quite probable. A similar conclusion was provided by Zhu et al. (2019) for karst caves in southwest China.

TABLE 5 Average values of the physico-chemical parameters (pH, EC) and ion contents (in mg/L) of the induced and natural condensation waters (see number of samples/measures in Tables 2 and 3) and of the rainwater (7 samples; 39 measures of pH and EC) in Nerja Cave for the studied period (2013–2018)

| Parameter/ion | Rainwater | Condensation water | |
|--------------------|-----------|--------------------|---------|
| | | Induced | Natural |
| pH | 7.62 | 7.82 | 7.74 |
| EC | 153 | 116 | 344 |
| HCO_3^- | 21.42 | 28.75 | 147.03 |
| Ca^{2+} | 5.28 | 18.95 | 24.23 |
| Mg^{2+} | 1.65 | 1.85 | 27.74 |
| Na^+ | 2.99 | 2.66 | 8.07 |
| K^+ | 0.70 | 0.83 | 2.10 |
| Cl^- | 5.64 | 2.28 | 9.71 |
| NO_3^- | 3.19 | 3.68 | 45.52 |
| SO_4^{2-} | 12.25 | 5.22 | 10.14 |
| PO_4^{3-} | 0.10 | 0.18 | 0.18 |
| F^- | 0.08 | 0.04 | 0.12 |
| TOC | – | 0.53 | 0.79 |
| SI Cal | – | –1.31 | –0.29 |
| SI Dol | – | –2.03 | 0.59 |
| PCO_2 | – | –3.37 | –2.53 |

Abbreviations: EC, Electrical conductivity (in $\mu\text{S}/\text{cm}$); PCO_2 , Partial pressure of CO_2 in equilibrium with the solution, expressed as $-\log \text{PCO}_2$; SI Cal, Calcite saturation index; SI Dol, Dolomite saturation index; TOC, Total organic carbon.

5.3 | Image analysis

Image analysis is part of a wider field known as image processing, where one of the main underlying ideas is to extract useful information or features. In this case, the aim was to evaluate the potential of this tool to extract quantitative information about the surface occupied by the condensation water and about its spatio-temporal variation.

In Nerja Cave, the first occurrence of condensation water in C2 (June) is linked to the onset of the summer ventilation regime, while its disappearance is related to the winter ventilation regime (Figure 6). During the summer, the natural ventilation of Nerja Cave is the lowest

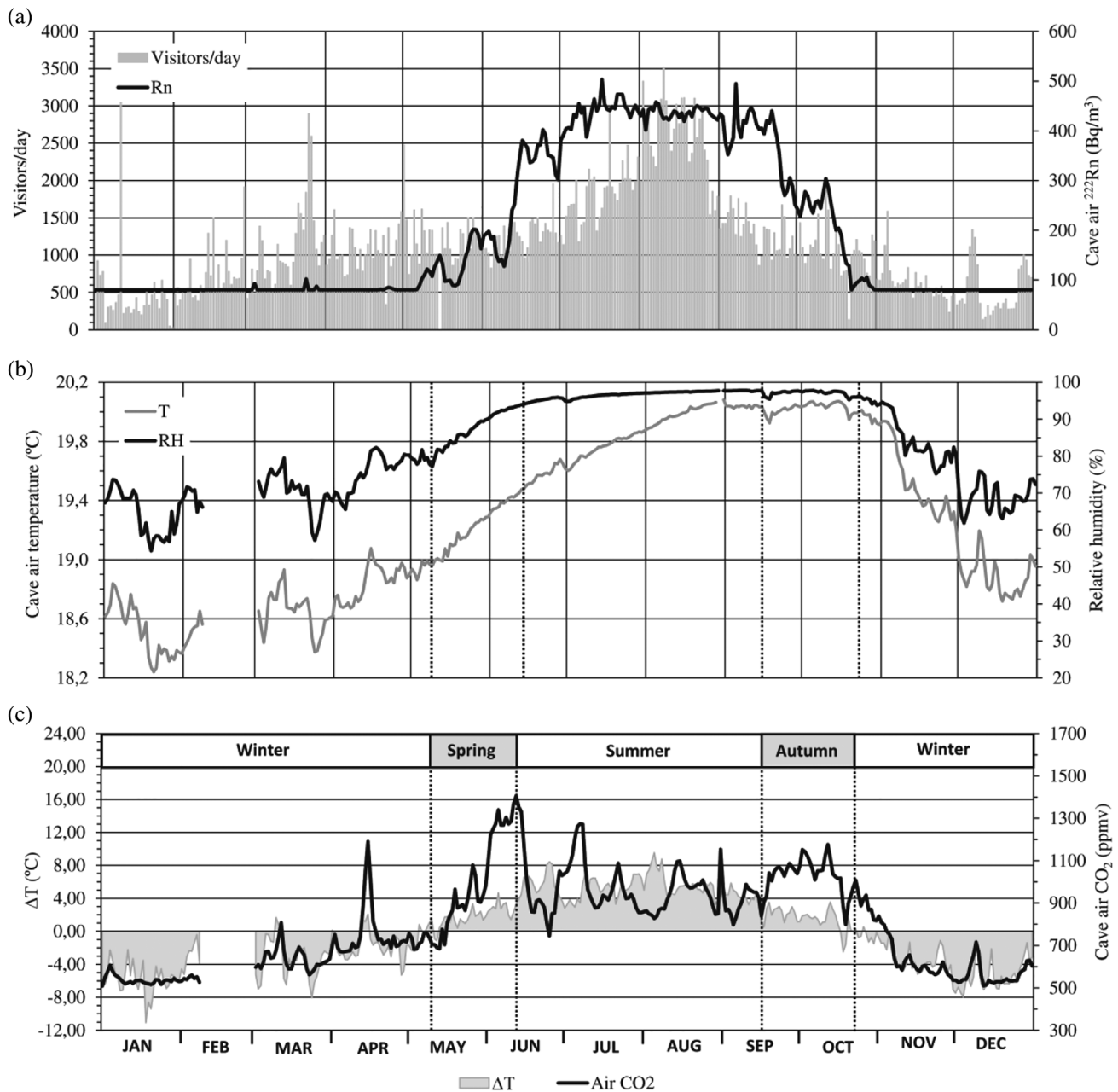


FIGURE 6 Daily evolution of (a) number of visitors in 2017 versus air ^{222}Rn concentration in H-2 (mean value for the period 2008–2013), (b) cave air temperature versus relative humidity (H-2) and (c) air CO_2 content (H-2) versus air temperature differences ($\Delta T = T_{\text{ext}} - T_{\text{int,H-2}}$) from 01 January 2017 to 31 December 17. Winter, spring, summer and autumn: Ventilation regimes defined in Nerja Cave

of the annual cycle, as indicated by the high gas ^{222}Rn concentration. The cave air, colder and denser than the external air, is expelled through its lowest entrances and external air is sucked in through the highest entrances. Thus, air arriving at C2 from June is warmer and more humid and originates from the non-visitable sector of the cave ($19.67^\circ\text{C}/98.55\%$ for June 2017). When this air arrives in the tourist sector where the temperature is cooler ($19.08^\circ\text{C}/92.16\%$ for the same period), water condenses due to the decrease of the saturation water vapour pressure in the air. The fact that condensation occurs in the ceiling of area C2 seems to be related to the lower air temperature of this sector (18.51°C), about 0.55°C lower than the temperature

recorded in chamber H-3 for the same period (19.16°C), according to the isolated measures performed in C2 from May to August 2018.

Thus, the analysis results show that the maximum surface occupied by the condensation water coincides with the period in which the cave air PCO_2 is higher, the relative humidity is at a maximum and the cave ventilation is minimal. In these conditions, the condensation water stays in contact with the rock and speleothems for longer, no evaporation processes exist or these are very limited and condensation water degassing is lower (minor gradient between water PCO_2 and air PCO_2), favouring the corrosion of speleothems and bedrock.

6 | CONCLUSIONS

This study has allowed us to identify and understand the hydrological processes that condensation water induces on cave substrates and their implications for the conservation of the speleothems and rock art. Condensation of water in cavities is one of the least addressed hydrological processes in the literature, regarding experimental data, due to the inherent difficulties in collecting representative water samples for chemical and isotopic analyses.

We determine the main isotopic and hydrochemical content of the condensation water (induced and natural) sampled in Nerja Cave, one of the most significant tourist and prehistoric sites of Europe. Seasonal variations of the isotopic composition, as opposed to the variations observed in the rainwater, have been detected in the induced condensation water. These are related to the more or less intense evaporation processes that occur inside the cave, depending on the degree of natural ventilation.

The higher HCO_3^- , Ca^{2+} and Mg^{2+} content in the natural condensation water with respect to induced condensation water evidence the existence of the “corrosion condensation” process of the carbonate walls and speleothems of the cave. In this study case, the areas occupied by the condensation water are highly localized, both spatially and temporally. These areas do not affect rock art, and thus the effect of the corrosion process is not significant with respect to heritage preservation. However, this study shows that the “condensation corrosion” process can potentially damage valuable heritage elements, like rock art and speleothems. This means that, in terms of cave conservation, especially in caves with substantial tourist activity, it is essential to control those factors that directly affect the condensation process and, thus, the corrosion of the rock substrate, such as temperature, humidity, and cave air CO_2 .

The high nitrate content found in the natural condensation water (up to 46 mg/L) has, most likely, a microbiological origin, associated with the presence of *Gammaproteobacteria* (*Nitrosococcaceae* family) in the rock substrate. We, therefore, rule out an origin related to activities or processes occurring outside the cave, where there are no industrial, agricultural, or livestock activities or a significant vegetal cover.

Our study shows the usefulness of image analysis techniques to quantify the surface occupied by the condensation water, and thus quantify the substrate surface potentially exposed to condensation corrosion processes, although additional studies are needed to improve the use of this methodology as a tool in the conservation of heritage sites.

ACKNOWLEDGEMENTS

This work is the result from the studies performed by the Geology area of the General Project for Interdisciplinary Research of the Nerja Cave, which is specifically aimed at the conservation of the cavity. The project is financed by the Nerja Cave Foundation, coordinated by its Research Institute and authorized by the Consejería de Cultura (Junta de Andalucía). The authors thank GeoTranslations for revising the English text, Manuela Vega for her support with

image analysis methodology and three anonymous reviewers who have contributed to improving this article. This work is a contribution to the Research Groups RNM-308 and RNM-126 of the Junta de Andalucía.

DATA AVAILABILITY STATEMENT

The data that support the findings of this study are available from the corresponding author upon reasonable request.

ORCID

Cristina Liñán  <https://orcid.org/0000-0003-3896-6647>

REFERENCES

- Alonso-Zarza, A. M., & Martín Pérez, A. (2008). Dolomite in caves: Recent dolomite formation in oxidic, non-sulfate environments. Castañar cave, Spain. *Sedimentary Geology*, 205(3–4), 160–164. ISSN 0037-0738. <https://doi.org/10.1016/j.sedgeo.2008.02.006>
- Andreo, B., Barberá, J. A., Mudarra, M., Marín, A. I., García-Orellana, J., Rodellas, V., & Pérez, I. (2018). A multi-method approach for groundwater resource assessment in coastal carbonate (karst) aquifers: The case study of sierra Almijara (southern Spain). *Hydrogeology Journal*, 26, 41–56. <https://doi.org/10.1007/s10040-017-1652-7>
- Andreo, B., & Carrasco, F. (1993). Estudio geoquímico de las aguas de infiltración de la Cueva de Nerja. In P. de la Cueva de Nerja & F. Carrasco (Eds.), *Geología de la Cueva de Nerja*, 3 (pp. 299–328). Patronato de la Cueva de Nerja.
- Andreo, B., Carrasco, F., Liñán, C., & Vadillo, I. (2002). Epigenic CO_2 controlling the drip water chemistry and speleothem growth in a Mediterranean karst area (Nerja cave, southern Spain). In Y. Daoxian & Z. Cheng (Eds.), *Karst processes and the carbon cycle* (pp. 51–64). Geological Publishing House.
- Aranburu, A., Bodego, A., Álvarez, I., Iriarte, E., Arriolabengoa, M., Bilbao, P., del Val, M., & Liñán, C. (2019). Estudio Geológico de la Cueva de Nerja (Málaga). Informe de actividades 2019, 18 p. Unpublished report.
- Auler, A. S., & Smart, P. L. (2004). Rates of condensation corrosion in speleothems of semi-arid northeastern Brazil. *Speleogenesis and Evolution of Karst Aquifers*, 2, 1–2.
- Avramidis, P., Hong, J., Barnes, C., & James, J. J. (2001). A new method of measuring condensation corrosion. Paper presented at: Proceeding of the 13th International Congress of Speleology, Brasilia (on cd).
- Badino, G. (2004). Clouds in caves. *Speleogenesis and Evolution of Karst Aquifers*, 2(2), 1–7.
- Benavente, J., Vadillo, I., Carrasco, F., Soler, A., Liñán, C., & Moral, F. (2010). Air carbon dioxide contents in the Vadose zone of a Mediterranean karst. *Vadose Zone Journal*, 9, 126–136. <https://doi.org/10.2136/vzj2009.0027>
- Cailhol, D., Audra, P., Nehme, C., Nader, F., Garasic, M., Heresanu, V., Gucel, S., Charalambidou, I., Satterfield, L., Cheng, H., & Edwards, R. (2019). The contribution of condensation-corrosion in the morphological evolution of caves in semi-arid regions: Preliminary investigations in the Kyrenia range, Cyprus. *Acta Carsologica*, 48(1), 5–27. <https://doi.org/10.3986/ac.v48i1.6782>
- Calaforra, J. M., Dell'Aglio, A., & Forti, P. (1993). The role of condensation-corrosion in the development of gypsum karst: The case of the Cueva dell'Agua (Sorbas, Spain). Paper presented at: XIth International Congress of Speleology, Guilin, China. pp. 63–66.
- Cañaveras, J. C., Sánchez-Moral, S., & Soler, V. (2001). Microorganisms and microbially induced fabrics in cave walls. *Geomicrobiology Journal*, 18, 223–240.
- Cardenal, J., Benavente, J., Andreo, B., & Carrasco, F. (1999). Modelización hidrogeoquímica del agua de infiltración en la Cueva de Nerja (Málaga). *Geogaceta*, 25, 63–65.

- Carrasco, F., Andreo, B., Liñán, C., & Mudry, J. (2006). Contribution of stable isotopes to the understanding of the unsaturated zone of a carbonate aquifer (Nerja cave, southern Spain). *Comptes Rendus Geoscience*, 338(16), 1203–1212. ISSN 1631-0713. <https://doi.org/10.1016/j.crte.2006.09.009>
- Casas, J., Martín de Vidales, J. L., Durán, J. J., López-Martínez, J., & Barea, J. (2001). Mineralogía de depósitos de tipo moonmilk en la Cueva de Nerja (Málaga, España). *Geogaceta*, 29, 29–32.
- Casas, J., Martín de Vidales, J. L., Durán, J. J., López-Martínez, J., & Barea, J. (2002). Presencia y mineralogía de depósitos de tipo moonmilk en la Cueva de Nerja (Málaga). In F. Carrasco, J. J. Durán, & B. Andreo (Eds.), *Karst and environment* (pp. 485–489). Fundación Cueva de Nerja.
- Cigna, A., & Forti, P. (1986). The speleogenetic role of air flow caused by convection. *International Journal of Speleology*, 15, 41–52.
- Craig, H. (1961). Standard for reporting concentration of deuterium and oxygen-18 in natural waters. *Science*, 133, 1702–1703.
- Cuezva, S. (2008). Dinámica microambiental de un medio kárstico somero (Cueva de Altamira, Cantabria): Microclima, geomicrobiología y mecanismos de interacción cavidad/exterior. Universidad Complutense. PhD tesis, 370.
- De Freitas, C. R., & Schmekal, A. (2003). Condensation as a microclimate process: Measurement, numerical simulation and prediction in the Glowworm cave, New Zealand. *International Journal of Climatology*, 23, 557–575.
- De Freitas, C. R., & Schmekal, A. (2006). Studies of corrosion/condensation process in the Glowworm cave, New Zealand. *International Journal of Speleology*, 35, 75–81.
- Dreybrodt, W., Gabrovsek, F., & Perne, M. (2005). Condensation corrosion: A theoretical approach. *Acta Carsologica*, 34(2), 34. <https://doi.org/10.3986/ac.v34i2.262>
- Dreybrodt, W., & Scholz, D. (2011). Climatic dependence of stable carbon and oxygen isotope signals recorded in speleothems: From soil water to speleothem calcite. *Geochimica et Cosmochimica Acta*, 75, 734–752.
- Dublyansky, V. N., & Dublyansky, Y. V. (1998). The problem of condensation in karst studies. *Journal of Cave and Karst Studies*, 60(1), 3–17.
- Dublyansky, V. N., & Dublyansky, Y. V. (2000). The role of condensation in karst hydrogeology and speleogenesis. In A. B. Klimchouk, D. C. Ford, A. N. Palmer, & W. Dreybrodt (Eds.), *Speleogenesis: Evolution of karst aquifers* (pp. 100–112). National Speleological Society.
- Dublyansky, Y. N., & Spötl, C. (2014). Morphological effects of condensation-corrosion speleogenesis at devils hole ridge, Nevada. In A. Klimchouk, I. D. Sasowsky, J. Mylroie, S. A. Engel, & A. S. Engel (Eds.), *Hypogene cave morphologies*. Karst Waters Institute Special Publication 18 ISBN Number: 978-0-9789976-7-0.
- Dueñas, C., Fernández, M. C., Cañete, S., Pérez, M., & Gordo, E. (2011). Seasonal variations of radon and the radiation exposure levels in Nerja cave, Spain. *Radiation Measurements*, 46, 1181–1186.
- Fairbridge, R. W. (1968). The Encyclopedia of geomorphology, In R. W. Fairbridge, (Ed.), *Encyclopedia of earth sciences series*, (Vol. 3, pp. 204–205). Dowden: Hutchinson & Ross.
- Fernández-Cortés, A., Calaforra, J. M., & García-Guinea, J. (2006). The Pulpí gigantic geode (Almería, Spain): Geology, metal pollution, microclimatology and conservation. *Environmental Geology*, 50, 707–716.
- Ferreira, T., & Rasband, W. (2012). ImageJ User Guide IJ 1.46r, 198 p.
- Forti, P., & Palmisano, G. (1989). I nitrati del Pulo di Molfetta: Mineralogia e meccanismi genetici Papr presented at: Proceedings of the 15th National Congress of Speleology, Castellana 1987, pp. 229–250.
- Galdenzi, S. (2012). Corrosion of limestone tablets in sulfidic groundwater: Measurements and speleogenetic implications. *International Journal of Speleology*, 41, 149–159.
- Gat, J. R., & Garmi, I. (1987). Effect of climate changes on the precipitation patterns and isotopic composition of water in a climate transition zone: Case of eastern Mediterranean Sea area. In *The influence of climate change and climatic variability on the hydrologic regime and water resources (proceedings of the Vancouver symposium)* (Vol. 168, pp. 513–523). IAHS Publications.
- Gázquez, F., Calaforra, J. M., Forti, P., De Waele, J., & Sanna, L. (2015). The role of condensation in the evolution of dissolutional forms in gypsum caves: Study case in the karst of Sorbas (SE Spain). *Geomorphology*, 229, 100–111. ISSN 0169-555X. <https://doi.org/10.1016/j.geomorph.2014.07.006>
- Hansen, M., Dreybrodt, W., & Scholz, D. (2013). Chemical evolution of dissolved inorganic carbon species flowing in thin water films and its implications for (rapid) degassing of CO₂ during speleothem growth. *Geochimica et Cosmochimica Acta*, 107, 242–251. ISSN 0016-7037. <https://doi.org/10.1016/j.gca.2013.01.006>
- Hill, C. A. (1987). Geology of Carlsbad cavern and other caves in the Guadalupe Mountains, New Mexico and Texas. *New Mexico Bureau of Mines and Mineral Resources Bulletin*, 117, 150.
- Hill, C. A., & Buecher, R. H. (1992). Nitrocalcite in Kartchner caverns, Kartchner caverns State Park, Arizona. *National Speleological Society Bulletin*, 54, 14–16.
- Hill, C. A., & Forti, P. (1997). *Cave minerals of the world* (2nd. ed., p. 463). National Speleological Society ISBN 1-879961-07-5.
- Holmes, A., Tujula, N., Holley, M., Contos, A., James, J., Rogers, P., & Gillings, M. (2001). Phylogenetic structure of unusual aquatic microbial formations in Nullarbor caves, Australia. *Environmental Microbiology*, 3, 256–264. <https://doi.org/10.1046/j.1462-2920.2001.00187.x>
- Homza, S., Rajman, L., & Roda, S. (1970). Vznik a vyvoj krasoveho fenomenu Ochtinskej aragonitovej jaskine. *Slovensky Kras*, 8, 21–68.
- Hoyos, M., Soler, V., Cañaveras, J. C., Sánchez-Moral, S., & Sanz-Rubio, E. (1998). Microclimatic characterization of a Karstic cave: Human impact on microenvironmental parameters of a prehistoric rock art cave Candamo cave, northern Spain. *Environmental Geology*, 33(4), 231–242.
- Istvan, D., & Micle, R. (1994). Calcite speleothems generated by underground evapocondensation (Pestera. Cobasel, Rodna Mountains). *Theoretical and Applied Karstology*, 7, 183–187.
- James, J. M., Jennings, J. N., & Dyson, H. J. (1982). Mineral decoration and weathering of the caves. In H. J. Dyson, R. Ellis, & J. M. James (Eds.), *Wombeyan caves* (p. 224). Sydney Speleological Society ISBN 0959960848, 9780959960846.
- Jiménez de Cisneros, C., Peña, A., Caballero, E., & Liñán, C. (2020). A multi-parametric approach for evaluating the current carbonate precipitation and external soil of Nerja cave (Málaga, Spain). *International Journal of Environmental Research*, 15(1), 1–13. <https://doi.org/10.1007/s41742-020-00278-x>
- Jordá, J. F., Aura, J. E., Álvarez, E., Avezuela, B., Badal, E., Maestro, A., Morales Pérez, J. V., Pérez Ripoll, M., & Villalba, M. P. (2011). Evolución paleogeográfica, paleoclimática y paleoambiental de la costa meridional de la Península Ibérica durante el Pleistoceno superior. El caso de la Cueva de Nerja (Málaga, Andalucía, España). *Boletín de la Real Sociedad Española de Historia Natural. Sección geológica*, 105(1–4), 137–147.
- Jurado, V., Hermosín, B., González- Pimentel, J. L., & Sáiz- Jiménez, C. (2018). Estudio molecular de dos áreas de crecimiento de microorganismos fototróficos y posibles agentes de su inhibición. Instituto de Recursos Naturales y Agrobiología de Sevilla (Agencia Estatal Consejo Superior de Investigaciones Científicas), 66 p. Unpublished report.
- Liñán, C., Andreo, B., Carrasco, F., & Vadillo, I. (1999). Hidrodinámica e hidroquímica de las aguas de goteo de la Cueva de Nerja. In B. Andreo, F. Carrasco, & J. J. Durán (Eds.), *Contribución del estudio científico de las cavidades kársticas al conocimiento geológico* (p. 592) ISBN 13: 9788492026869. Patronato de la Cueva de Nerja.
- Liñán, C., Andreo, B., Carrasco, F., & Vadillo, I. (2000). Consideraciones acerca de la influencia del CO₂ en la hidroquímica de las aguas de goteo de la Cueva de Nerja (Provincia de Málaga). *Geotemas*, 3(1), 341–344.
- Liñán, C., Ojeda, L., Benavente, J., del Rosal, Y., Vadillo, I., & Carrasco, F. (2020). Coupling air temperature records and gravimetric data to

- interpret ventilation patterns in a Mediterranean karstic system (Nerja-Pintada caves, southern Spain). *Science of the Total Environment*, 730, 139147, ISSN 0048-9697. <https://doi.org/10.1016/j.scitotenv.2020.139147>
- Liñán, C., del Rosal, Y., Cantos, F., Vadillo, I., Benavente, J., & Ojeda, L. (2018). Highlighting the importance of transitional ventilation regimes in the management of Mediterranean show caves (Nerja-Pintada system, southern Spain). *Science of the Total Environment*, 631-632, 1268-1278. <https://doi.org/10.1016/j.scitotenv.2018.02.304>
- Liñán, C., Simón, M. D., del Rosal, Y., & Garrido, A. (2007). Estudio preliminar del clima en el entorno de la Cueva de Nerja (Andalucía, provincia de Málaga). In J. J. Durán, P. Robledo, & J. Vázquez (Eds.), *Cuevas turísticas: Aportación al desarrollo sostenible* (Vol. 24, pp. 159-168). Publicaciones del IGME, serie Hidrogeología y aguas subterráneas.
- Martínez-Arkarazo, I., Angulo, M., Zuloaga, O., Usobiaga, A., & Madariaga, J. (2008). Spectroscopic characterisation of moonmilk deposits in Pozalagua tourist cave (Karrantza, Basque Country, north of Spain). *Spectrochimica Acta. Part A, Molecular and Biomolecular Spectroscopy*, 68, 1058-1064. <https://doi.org/10.1016/j.saa.2007.05.026>
- Martín-García, R., Martín-Pérez, A., & Alonso-Zarza, A. (2010). Petrological study as a tool to evaluate the degradation of speleothems in touristic caves, Castañar de Ibor cave, Cáceres, Spain. In B. Andreo, F. Carrasco, J. Durán, & J. LaMoreaux (Eds.), *Advances in research in karst media. Environmental earth sciences*. Springer. https://doi.org/10.1007/978-3-642-12486-0_78
- Morat, P., & Le Mouél, J. L. (1992). Electrical signals generated by stress variations in porous non-saturated rocks. *Comptes Rendus Académie Science Paris*, 315, 955-963.
- Palmer, A. N., & Palmer, M. V. (2000). Speleogenesis of the Black Hills maze caves, South Dakota, U.S.A. In A. B. Klimchouk, D. C. Ford, A. N. Palmer, & W. Dreybrodt (Eds.), *Speleogenesis: Evolution of karst aquifers* (pp. 274-281). National Speleological Society.
- Prokofiev, S. S. (1964). The role of condensation moisture in creation of Karst caves. *Peshcheri, Perm.* 4 (5), pp. 35-38.
- Quiles, A., Fritz, C., Medina, M. A., Pons-Branchu, E., Sanchidrián, J. L., Tosello, G., & Valladas, H. (2014). Chronologies croisées (C-14 et U/Th) pour l'étude de l'art préhistorique dans la grotte de Nerja: Méthodologie. In M. A. Medina-Alcaide, A. J. Romero, R. M. Ruiz-Márquez, & J. L. Sanchidrián (Eds.), *Sobre rocas y huesos* (pp. 420-427) ISBN: 978-84-617-2993-7. Fundación Cueva de Nerja & Universidad de Córdoba.
- Reyes, E., Caballero, E., Rodríguez, P., Jiménez de Cisneros, C., & Delgado, A. (1993). Caracterización isotópica y análisis de los procesos de degradación de los materiales carbonatados de la Cueva de Nerja. In F. Carrasco (Ed.), *Geología de la Cueva de Nerja*, 3 (pp. 265-296). Patronato de la Cueva de Nerja.
- Rogerio-Candelera, M. A., Laiz, L., González, J. M., & Sáiz-Jiménez, C. (2008). Monitorización del crecimiento microbiano en una tumba romana mediante técnicas de teledetección. In M. García, I. Montero, & S. Rovira (Eds.), *Actas del VII Congreso Ibérico de Arqueometría* (pp. 593-600). Consejo Superior de Investigaciones Científicas.
- Sánchez-Moral, S., Cuezva, S., Fernández-Cortes, A., Janices, I., Benavente, D., Cañaveras, J. C., González Grau, J. M., Jurado, V., Trobajo, L. L., Guisado, M., Candelera, M. A. R., & Sáiz-Jiménez, C. (2014). Estudio integral del estado de conservación de la cueva de Altamira y su arte paleolítico (2007-2009). Perspectivas futuras de conservación. Monografías. N° 24. Museo Nacional y Centro de Investigación de Altamira, 397 p.
- Sánchez-Moral, S., Soler, V., Cañaveras, J. C., Sanz-Rubio, E., Van Grieken, R., & Gysels, K. (1999). Inorganic deterioration affecting the Altamira cave, N Spain: Quantitative approach to wall-corrosion (solutional etching) processes induced by visitors. *Science of the Total Environment*, 243-244, 67-84. [https://doi.org/10.1016/s0048-9697\(99\)00348-4](https://doi.org/10.1016/s0048-9697(99)00348-4)
- Sanna, L., De Waele, J., Calaforra, J., & Forti, P. (2015). Long-term erosion rate measurements in gypsum caves of Sorbas (SE Spain) by the micro-erosion meter method. *Geomorphology*, 228, 213-225. <https://doi.org/10.1016/j.geomorph.2014.09.009>
- Sarbu, S. M., & Lascu, C. (1997). Condensation corrosion in Movile Cave, Romania. *Journal of Caves and Karst Studies*, 59, 99-102.
- Spötl, C., Fairchild, I., & Tooth, A. (2005). Cave air control on dripwater geochemistry, Obir caves (Austria): Implications for speleothem deposition in dynamically ventilated caves. *Geochimica et Cosmochimica Acta*, 69, 2451-2468. <https://doi.org/10.1016/j.gca.2004.12.009>
- Tarhule-Lips, R. F. A., & Ford, D. C. (1998). Condensation corrosion in caves on Cayman Brac and Isla de Mona. *Journal of Caves and Karst Studies*, 60, 84-95.
- Thornbush, M. J., & Viles, H. A. (2008). Photographic monitoring of soiling and decay of roadside walls in Central Oxford, England. *Environmental Geology*, 56(3-4), 777-787.
- Vadillo, I. (2010). Caracterización del comportamiento hidrogeológico y estudio de las variaciones de parámetros atmosféricos en la cavidad de Praileaitz (Bajo Deba, Gipuzkoa). Universidad de Málaga, 46 p. Unpublished report.
- Vadillo, I., Benavente, J., Liñán, C., Carrasco, F., & Soler, A. (2016). Nuevos datos hidroquímicos e isotópicos en el manantial kárstico de Maro (Nerja, Málaga). Consideraciones sobre el origen de los solutos y de la influencia de la ventilación en la zona vadosa. *Geogaceta*, 59, 47-50.
- Vieten, R., Winter, A., Samson, A., Cooper, J., Wrapson, L., Kambesis, P., Lace, M., & Nieves, M. (2016). Quantifying the impact of human visitation in two cave chambers on Mona Island (Puerto Rico): Implications for archaeological site conservation. *Cave and Karst Science*, 43, 79-85.
- Wolery, T. J. (2013). EQ3/6 - Software for Geochemical Modeling, Version 8.0a, LLNL-CODE-2013-683958, Lawrence Livermore National Laboratory, Livermore, CAL
- Zhu, H.-Z., Zhang, Z.-F., Zhou, N., Jiang, C.-Y., Wang, B.-J., Cai, L., & Liu, S.-J. (2019). Diversity, distribution and co-occurrence patterns of bacterial communities in a karst cave system. *Frontiers in Microbiology*, 10, 1726. <https://doi.org/10.3389/fmicb.2019.01726>

How to cite this article: Liñán C, Benavente J, del Rosal Y, Vadillo I, Ojeda L, Carrasco F. Condensation water in heritage touristic caves: Isotopic and hydrochemical data and a new approach for its quantification through image analysis. *Hydrological Processes*. 2021;35:e14083. <https://doi.org/10.1002/hyp.14083>